3-11-2011

Modeling Enhanced Storage of Groundwater Contaminants Due to the Presence of Cracks in Low Permeability Zones Underlying Contaminant Source Areas

Jeremy M. Miniter

MODELING ENHANCED STORAGE OF GROUNDWATER CONTAMINANTS DUE TO THE PRESENCE OF CRACKS IN LOW PERMEABILITY ZONES UNDERLYING CONTAMINANT SOURCE AREAS

THESIS

Jeremy M. Miniter, Captain, USAF
AFIT/GES/ENV/11-M02

DEPARTMENT OF THE AIR FORCE
AIR UNIVERSITY
AIR FORCE INSTITUTE OF TECHNOLOGY

Wright-Patterson Air Force Base, Ohio

The views expressed in this thesis are those of the authors and do not reflect the official policy or position of the United States Air Force, Department of Defense or the United States Government.

AFIT/GES/ENV/11-M02

MODELING ENHANCED STORAGE OF GROUNDWATER CONTAMINANTS DUE TO THE PRESENCE OF CRACKS IN LOW PERMEABILITY ZONES UNDERLYING CONTAMINANT SOURCE AREAS

THESIS

Presented to the Faculty

Department of Systems and Engineering Management

Graduate School of Engineering and Management

Air Force Institute of Technology

Air University

Air Education and Training Command

In Partial Fulfillment of the Requirements for the

Degree of Master of Science in Environmental Engineering and Science

Jeremy M. Miniter, BS

Captain, USAF

March 2011

AFIT/GES/ENV/11-M02

MODELING ENHANCED STORAGE OF GROUNDWATER CONTAMINANTS DUE TO THE PRESENCE OF CRACKS IN LOW PERMEABILITY ZONES UNDERLYING CONTAMINANT SOURCE AREAS

Jeremy M. Miniter, BS

Captain, USAF

Approved:

//signed//	11 Mar 2011
Mark N. Goltz, Ph.D. (Chairman)	Date
//signed//	9 Mar 2011
Avery H. Demond, Ph.D. (Member) University of Michigan	Date
//signed//	7 Mar 2011
Junqi Huang, Ph.D. (Member) U.S. Environmental Protection Agency	Date

Abstract

Throughout the Air Force and DoD, chlorinated aliphatic hydrocarbons (CAHs), which are a type of Dense Non-Aqueous Phase Liquid or "DNAPL," have been frequently used. Their disposal has led to subsurface soil and groundwater contamination. DNAPLs move through soils and groundwater, leaving behind residual separate phase contamination as well as pools atop low permeability layers. DNAPL contamination is difficult to clean up with existing environmental remediation technologies. In this study a numerical model constructed using the DoD Groundwater Modeling System (GMS) is used as a tool to assess how cracks in a low permeability layer, either pre-existing or resulting from the interaction between a DNAPL pool and the layer, might ultimately impact the longevity of a dissolved phase CAH plume that will be generated by the DNAPL source. The conceptual model posits a DNAPL source in a high permeability sand layer is sitting atop a low permeability clay layer. The model simulates DNAPL dissolving into groundwater flowing through the sand, and assumes the dissolved CAH is transported by the processes of advection, dispersion, and sorption. These transport processes in the sand are coupled to processes occurring in the low permeability clay. Dissolved phase CAH is assumed to be transported by diffusion in the clay. However, due to the presence of cracks in the clay, there may be "enhanced diffusion" of dissolved phase CAH in the clay due to advective transport in the cracks. Advective transport in the cracks coupled to diffusive transport in the clay matrix is simulated using a dual domain model. Model results indicate that as the cracking increases, there is an increase in the mass of contaminant that enters and is stored in the

clay. This leads to higher concentrations of contaminant that “back diffuses” out of the clay, resulting in higher downgradient plume concentrations (known as “tailing”) long after the contaminant source has been removed.

Acknowledgments

I appreciate the opportunity my thesis adviser, Dr. Mark N. Goltz, gave me by allowing me to work with him on this thesis topic and thank him for all the guidance and support he provided. I also appreciate the GMS modeling guidance and support that Dr. Junqi Huang at Robert S. Kerr Environmental Research Center provided and thank him for agreeing to be one of my thesis committee members. I would also like to thank my other thesis committee member, Dr. Avery H. Demond at the University of Michigan, for serving as my other committee member and providing guidance and support.

I would also like to thank the Strategic Environmental Research and Development Program (SERDP) for providing financial support for this research and also the staff of the Air Force Institute of Technology Library for providing guidance and support during the literature review process.

Jeremy M. Miniter

Table of Contents

Page

Page

List of Figures

Page

List of Tables

Page

MODELING ENHANCED STORAGE OF GROUNDWATER CONTAMINANTS DUE TO THE PRESENCE OF CRACKS IN LOW PERMEABILITY ZONES UNDERLYING CONTAMINANT SOURCE AREAS

1.0 Introduction

1.1 Background

Throughout the Air Force and the Department of Defense (DoD), chlorinated solvents such as trichloroethylene (TCE) and tetrachloroethylene (PCE), which are classified as Dense Non-Aqueous Phase Liquids (DNAPLs), have been used as cleaning solutions to clean items as diverse as aircraft and motor vehicle parts and clothing (PCE is commonly used for dry-cleaning). Before environmental regulations were in place banning the improper disposal of these solvents, they were often disposed of in sanitary and storm sewers, disposal pits, and fire training areas. Disposal in this manner has led to subsurface soil and groundwater contamination. DNAPLs are denser than, and only slightly soluble in, water. Due to their density, DNAPLs move vertically through soils and groundwater until their downward movement is impeded by low permeability layers. The DNAPL will then pool atop the low permeability layers. Figure 1 is a conceptual illustration showing DNAPL migration in the subsurface. Particularly note the DNAPL that has pooled atop the two low permeability layers.

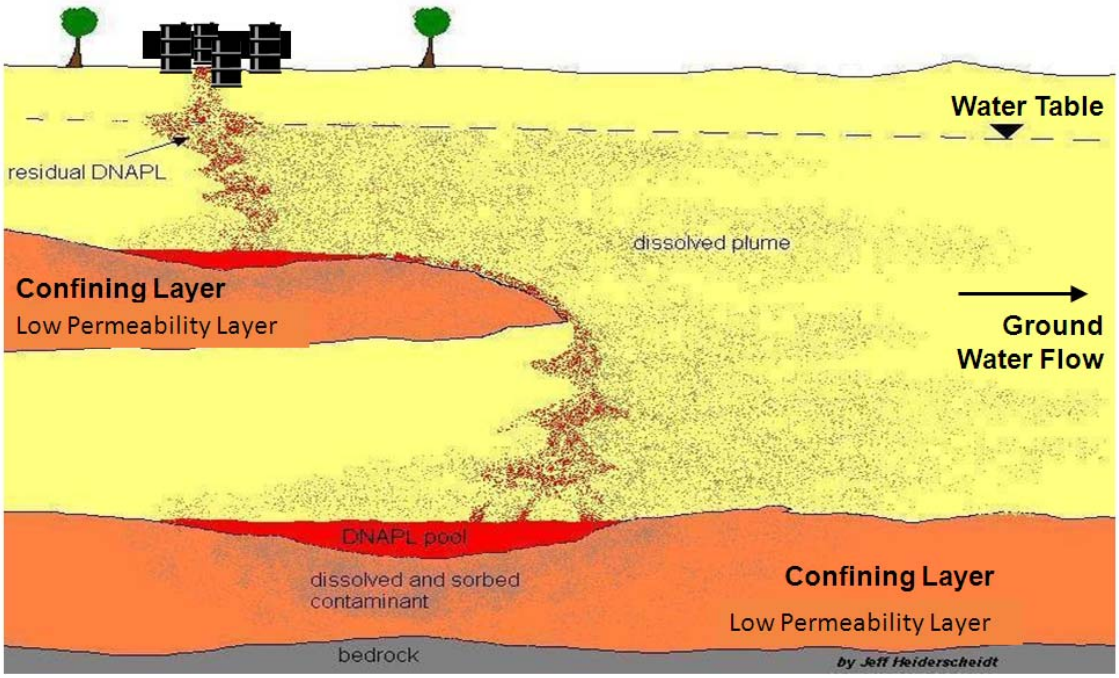

Figure 1: DNAPL Movement in the Subsurface (after Heiderscheidt, 2010)

Due to the large amount of chlorinated solvents that the DoD and industry have used and disposed of over the years, both properly and improperly, chlorinated solvent contamination is an important issue. The U.S. Environmental Protection agency (EPA) estimates that 60% of Superfund sites across the United States are contaminated with DNAPLs (U.S. EPA, 2010).

Methods of remediating DNAPL source areas, such as surfactant/cosolvent flushing or in situ chemical oxidation/reduction, involve introducing a solution into the subsurface in order to solubilize, mobilize, or chemically react with the NAPL. The introduced solution flows through the high permeability zones, and typically does not interact with DNAPL stored in the low permeability layers. Thus, even though DNAPL may have been removed from the high permeability zones, the low permeability layers serve to store DNAPL. Thus a concentration gradient is established; high concentrations

in the low permeability zones, and low concentrations in the high permeability zones, which have been remediated. Because of the concentration gradient, DNAPL can then diffuse back from the low permeability layers into the high permeability zones. This is known as "back diffusion."

The storage of DNAPLs in low permeability lenses and layers in the subsurface creates long-term contaminant sources. As this storage limits the ability of remediation technologies to meet cleanup goals, and impacts the longevity of groundwater contamination plumes, it is necessary that we develop a better understanding of the storage process. It is thought that contaminant movement into these low permeability lenses and layers occurs primarily through the process of transverse diffusion (Ball et al., 1997; AFCEE, 2007; Parker et al., 2008). However, there is also evidence that either advective transport or enhanced diffusive transport occurs, as reported contaminant concentrations in these low permeability zones can be greater than that which can be accounted for by diffusion alone (AFCEE, 2007). This enhanced transport may be due to naturally occurring cracks present in the low permeability zone or cracking due to DNAPL that has pooled atop the low permeability zone. The interaction between the DNAPL and low permeability zone may affect the properties of the clay comprising the low permeability zones, thereby promoting enhanced transport of the DNAPL into these zones (Ayral et al., 2010). It has been reported that the hydraulic conductivity of common clay minerals can be one to five orders of magnitude times greater when permeated by organic liquids than when permeated by water, depending on the organic liquid, and the fraction and type of clay (Brown and Thomas, 1987). This increase in hydraulic conductivity has been ascribed to interlayer compression (Li et al., 1996).

Essentially, contact with organic liquids causes the clay structure to shrink, leading to the formation of cracks and microfractures and a concomitant increase in hydraulic conductivity (Brown and Thomas, 1987). Current modeling approaches looking at the transport of contaminants into and out of clay layers and lenses, such as those utilized by Ball et al. (1997), Parker et al. (2008), and Sale et al. (2008) treat the process as diffusion in a dilute solution, modified by a tortuosity factor to account for the reduced area and the increased transport path length in a porous medium. This approach does not account for the cracks in the clay, which may be pre-existing or the result of interactions between DNAPL pools and low permeability layers and lenses. As discussed above, the impact of these interactions may be significant (e.g., Brown and Thomas, 1987). Not accounting for the altered clay structure, and the ensuing enhanced transport into these low permeability layers that might result, could lead to significantly erroneous predictions of storage in the low permeability zones and the rates at which the DNAPLs enter into and are released from these zones. If the analysis of site remediation options are then based on the faulty predictions of storage and transport, inappropriate strategies may be recommended for managing the site.

Researchers at the Air Force Institute of Technology (AFIT), in collaboration with researchers at the University of Michigan, have proposed to model the enhanced transport and storage of groundwater contaminants in low permeability layers that underlie a contaminant source area. The researchers at the University of Michigan will focus on experimentally studying how low permeability soil materials are modified in the presence of both pure DNAPLs and DNAPLs with surfactants. It was proposed that these experimental results would then be used by AFIT researchers to model the effect of

DNAPLs on low permeability materials, and ultimately apply the model to simulate (1) the transport of DNAPL compounds into and out of the low permeability zones, and (2) the evolution of dissolved phase contaminant plumes from the low permeability source.

Throughout this chapter and in subsequent chapters any reference to DNAPL will be for the separate, immiscible phase. The dissolved contaminant phase will be defined and referred to as dissolved CAH.

1.2 Research Objective

The primary objective of this research is to develop a model that demonstrates enhanced transport of groundwater contaminants into and out of a low permeability layer from a DNAPL source atop the layer and simulate how this enhanced transport might affect the evolution and longevity of the dissolved phase plume. The enhanced transport is assumed to be the result of cracks in the low permeability layer.

1.3 Specific Research Questions

1. What processes occur when DNAPLs and low permeability layers interact?
2. What is the effect of cracking on the transport of DNAPLS into and out of low permeability layers?
3. What mathematical models are available that can be used to model diffusion and enhanced diffusion into low permeability layers?
4. What mathematical models can be used to simulate other processes (e.g., advection, dispersion, diffusion) that have been found to contribute to enhanced transport of the DNAPL into the low permeability layer?

5. What is the effect of enhanced transport into low permeability layers on dissolved plume longevity and evolution?

1.4 Research Approach

The initial phase of the study involves a literature review to: 1) determine the appropriate set of mathematical equations that can be used to model diffusion into low permeability zones; 2) learn what processes occur when DNAPLs and low permeability layers interact; 3) determine the appropriate set of mathematical equations that can be used to model enhanced diffusion into low permeability zones.

The second phase of the study involves coupling diffusion and enhanced diffusion submodels with "standard" dissolved contaminant transport models (advection-dispersion equations) and use the coupled model to simulate the effect of enhanced diffusion on plume longevity and growth.

1.5 Scope and Limitation of Research

Parameter values used in the enhanced diffusion model are "guesstimated" based on the literature. No "real world" remediation site data are available to validate the model. Also, the model developed in this study is a simplified model that assumes (1) a sorbing, but otherwise conservative contaminant (no degradation), (2) the subsurface material properties are homogeneous in space and time; (3) steady state flow. Also note that the model simulates dissolved contaminant transport only; the DNAPL source is assumed to be immobile. These assumptions are made so that the effect of enhanced diffusion on plume evolution can be focused on. Finally the concentration versus time breakthrough data, which are used to study plume longevity, are simulated at a single

observation point downgradient from the DNAPL source. Different concentration versus time data would be simulated if the observation point were moved closer or further from the DNAPL source. Nevertheless, it is assumed that the overall plume behavior can be understood, at least in a qualitative sense, by observing the breakthrough behavior at a representative downgradient observation point

1.6 Definition of Terms

Advection - fluid transport due to fluid motion

Basal spacing - spacing between adjacent layers of a crystalline structure

Crack - an opening in a material caused by an applied stress that allows fluid to freely enter the material

Dense Non-aqueous Phase Liquid (DNAPL) - a liquid that is denser than water and also immiscible in water.

Dielectric Constant (E) - ratio of the permittivity of a material to the permittivity of a vacuum. Low E materials have a low ability to polarize and hold a charge and thus have low permittivity.

Diffusion - movement of a dissolved solute caused by a concentration gradient

Dispersion - spreading of mass beyond a region it normally would occupy due to advection alone

Electrophoteric potential - movement of particles under an applied electric field.

Enhanced Diffusion - diffusion from cracks in a material that allows increased mass to enter the material due to the presence of the cracks

Hydraulic conductivity – the factor of proportionality between specific discharge and hydraulic gradient

Permeability- the ease with which fluid can move through porous material

Permittivity - measure of a materials ability to be polarized by an electric field.

Zeta potential - a calculated value that indicates the degree of repulsion between two adjacent, similarly charged particles.

2.0 Literature Review

2.1 Overview

Groundwater contaminants, such as chlorinated aliphatic hydrocarbons (CAHs), stored in subsurface low permeability layers pose long term challenges for remediation. It is estimated that over 3,000 Department of Defense (DOD) sites are contaminated with various CAHs which were used as solvents (SERDP, 2008). Dissolved-phase plumes tend to be large and can extend for miles downgradient from the original contamination source. Contamination plumes that contain CAHs are difficult to remediate due to the relatively high solubility and limited retardation of CAH transport due to sorption (SERDP, 2008). The ability of low permeability layers to store CAHs further hinders the CAH contamination remediation effort. In a situation where high permeability layers, which could serve as drinking water sources, are contaminated with CAHs, and the subsurface also consists of low permeability layers, these low permeability layers can act as CAH contamination sources after the high permeability zones are remediated. This process of aquifer recontamination is caused by the back diffusion of the CAH from the low permeability layer to the high permeability layer. This back diffusion is caused by the concentration gradient that is set up between the clean high permeability layer and the contaminated low permeability layer.

A better understanding of the impact that chlorinated solvents stored in low permeability layers has is needed to improve the ability to reach groundwater cleanup goals. The CAHs that are the focus of this research are dense nonaqueous phase liquids (DNAPLs) like trichloroethylene (TCE).

2.2 Transport of Dissolved Compounds in Low Permeability Materials

The primary transport mechanism for dissolved contaminants in low permeability layers, where advection is negligible, is simple Fickian diffusion. Johnson et al. (1989) used field data collected from a waste disposal facility in Ontario to show that transport by simple Fickian diffusion is more important than advective transport when assessing the transport of contaminants into low permeability layers. Core samples were collected from an unweathered clay deposit beneath a five year old hazardous waste landfill and analyzed for chlorides and volatile organic compounds. A plot of chloride concentration versus depth below the landfill/clay interface showed that the maximum depth that the chloride was transported was 83 cm. The plot showed the chloride concentration decreasing with distance and suggested chloride transport was due to "classic diffusion" (Johnson et al., 1989). Using mathematical modeling the authors were able to confirm that the dominant chloride transport mechanism was diffusion in accordance with Equation 2.1, Fick's second law,

$$\frac{\partial C}{\partial t} = D_{eff}\frac{\partial^2 C}{\partial y^2} \qquad \text{(Eq 2.1)}$$

where C is concentration [ML^{-3}], D_{eff} [L^2T^{-1}] is the effective diffusion coefficient, and y [L] is the vertical coordinate, with the positive direction downwards. The effective diffusion coefficient (D_{eff}) is related to the free-solution diffusion coefficient (D_0) by the following equation:

$$D_{eff} = D_o\tau \qquad \text{(Eq 2.2)}$$

where τ is a tortuosity factor ($0<\tau<1$) that accounts for the tortuous nature of the clay material (Clark, 2009).

The organic compounds were only detected down to a depth of 15cm. The concentration versus depth data for the organic compounds also could be simulated assuming Fickian diffusion. Sorption of the organic compounds to the clay particles was assumed to play an important role in retarding the movement of the organic compounds through the low permeability layer (Johnson et al., 1989).

The effect of sorption of the organic compounds to the clay particles can be incorporated into the diffusion equation by modifying the effective diffusion coefficient

$$D'_{eff} = \frac{D_o \tau}{R_{imm}} \quad \text{(Eq 2.3)}$$

where R_{imm} [-] is a retardation factor that accounts for linear, equilibrium sorption of the organic compound to the clay immobile phase:

$$R_{imm} = 1 + \frac{\rho_b K_d}{\theta} \quad \text{(Eq 2.4)}$$

where ρ_b [ML^{-3}] is the bulk density of clay, θ [-]is the porosity of clay, and K_d [$M^{-1}L^3$] is the sorption partition coefficient of dissolved organic compound (Clark, 2009).

Parker et al. (2004) conducted a field study at an industrial site in Connecticut to determine the integrity of a 20-m-thick clayey silt aquitard that had an accumulated pool of free-product trichloroethylene (TCE) dense non-aqueous phase liquid (DNAPL) atop it. From 1952 to 1972 TCE was used at the facility for degreasing operations. It was assumed that residual and free-product TCE started pooling atop the aquitard sometime in the 1950s. The sand aquifer below the aquitard was pumped in order to provide water to the site from the 1950s to 2001. Parker et al. (2004) proposed that TCE could be transported into the aquitard by one or more of the following processes: (1) bulk movement of the DNAPL (free-product TCE), (2) advection of dissolved TCE due to the

hydraulic gradient established by pumping the lower aquifer, and/or (3) diffusion of dissolved TCE. The researchers sampled for dissolved and/or separate phase TCE in the aquitard, in order to ascertain the primary transport processes within the low permeability clayey silt.

Cores collected from the aquitard indicated the presence of TCE at a depth of 2.5 to 3 m below the top of the aquitard (Parker et al., 2004). These results were compared to the results of one-dimensional analytical and numerical solutions of TCE migration in the aquitard which showed downward migration of aqueous TCE to a depth of 4 to 5 m into the aquitard (Parker et al., 2004). Cases assuming diffusion only and diffusion and advection were compared. Based on measured TCE concentration values and the results of the one-dimensional model simulations, the conclusion was that diffusion of aqueous TCE is the dominant transport process in the clayey silt aquitard and that advection, due to the hydraulic gradient established by pumping the underlying aquifer, was negligible.

2.3 Back Diffusion

As stated previously, back diffusion can occur when a concentration gradient is established between an uncontaminated high permeability zone and a contaminated low permeability zone. Parker et al. (2008) showed that back diffusion from an aquitard in a sand aquifer could cause contaminant persistence above MCLs long after the contaminant plume source zone was isolated or removed.

Wilson (1997) studied how pump-and-treat systems used to remediate contaminated aquifers have failed to restore aquifers to drinking water standards. Aquifer heterogeneities (i.e., numerous high and low permeability zones interspersed in

the aquifer) were identified as one possible explanation why pump-and-treat systems fail. Contaminant concentrations at pumping wells used to capture plumes typically drop to low levels, where they level off. On concentration versus time breakthrough curves constructed from measurements of concentration in water extracted at the pumping well, this appears as a long-lasting low concentration tail. When pumping is stopped for a time and then resumed, concentration levels are often found to have risen (so-called rebound). Tailing and rebound of contaminant concentrations at extraction wells during pump-and-treat remediation are often attributed to slow back diffusion of stored contaminant from low permeability zones within the aquifer (Wilson, 1997).

Liu and Ball (2002) studied the diffusion of tetrachloroethene (PCE) and TCE in a natural aquitard below Dover Air Force Base, Delaware. At this Dover Air Force Base site bentonite-sealed steel sheetpiles were installed to establish two experimental test cells that hydraulically isolated the contaminated aquifer and aquitard from the surrounding groundwater flow. The sheetpiles were installed to a depth of approximately 2.0 m into the aquitard. The aquifer and aquitard had been exposed to water contaminated with dissolved (but not DNAPL) PCE and TCE for more than a decade (Mackay et al., 2000). Three injection and three extraction wells were installed in each of the two cells. One test cell was subjected to continuous pumping and the other test cell was subjected to pulsed pumping. Over a 35 month period the test cells were subjected to no-flow conditions for 11.1 months followed by 8.1 months of pumping followed by 15.8 months of no-flow conditions. Throughout the 35 month period, core samples were collected from the test cells and analyzed for PCE and TCE content. The pumping conducted within the two test cells and the no-flow conditions following the pumping

established the necessary conditions to promote back diffusion of contaminants from the aquitard into the aquifer (Liu and Ball, 2002).

Sorption and diffusion data were obtained in the laboratory. These data were used in a model that assumed sorption-retarded diffusion of TCE and PCE within the aquitard. Model simulations were run with these independently determined parameters. The model predicted concentrations were compared with coring results and close agreement was found. The authors concluded that diffusion, not advection or transformation, was the dominant transport process occurring in the aquitard (Liu and Ball, 2002).

Chapman and Parker (2005) investigated how back diffusion from a clayey silt aquitard caused the persistence of a TCE plume 330 m downgradient from the TCE source, even though the source itself was isolated in 1994 by the installation of a sheet piling enclosure. This investigation took place at the same industrial site in Connecticut that Parker et al. (2004) reported on in their investigation of TCE diffusion in the clay aquitard. Data from aquitard cores helped determine the contaminant distribution in the aquitard below the plume and groundwater data collected from a site-wide network of conventional monitoring wells helped determine the concentration of TCE in the groundwater downgradient from the DNAPL source.

Seven to ten months after the DNAPL source was isolated, data from two of the monitoring wells 330 m down gradient from the isolated DNAPL source indicated a substantial decrease in TCE concentrations. The TCE concentration decreased from between 5000 to 30,000 µg/L to between 200 to 3000 µg/L 2.5 years after installation of the sheet pile enclosure.

The time between the sheet piling installation to isolate the source zone and the TCE concentration decline at the downgradient monitoring well was in close agreement to the travel times determined using the velocity calculated by Darcy's Law and measured by borehole dilution. This agreement confirms that the TCE concentration decline was caused by the isolation of the DNAPL source zone (Chapman and Parker, 2005). Due to the low organic carbon content of the aquifer sand, TCE retardation was assumed negligible.

A decade after the DNAPL source isolation, a "tail" of persistent, low TCE concentrations were measured in the two monitoring wells downgradient from the sheet pile enclosure. The conclusion was that sources of TCE outside of the enclosure existed. Three hypotheses about the source of the TCE were proposed. The first hypothesis was that back diffusion of TCE from the aquitard below the plume was occurring. The second hypothesis was that a small area of DNAPL contamination which had been found outside the enclosure was the source of the TCE. The last hypothesis was that there was some other unknown/unidentified DNAPL source zone outside the enclosure. Numerical modeling was used to show that back diffusion fully accounted for the plume tailing (Chapman and Parker, 2005).

Similar to the study presented in Parker et al. (2004) of the industrial site in Connecticut, Parker et al. (2008) is an investigation of an industrial site in Florida that had an aquifer contaminated with TCE. This site was near a metal fabricating and precision cleaning facility that used TCE as a solvent. The site's TCE contamination was estimated to have occurred from the mid- to late 1960s to 1977. The aquifer below the site was described as heterogeneous with beach sand deposits and thin laterally

discontinuous silt and clay lenses. A 5 to 20 cm thick clay layer runs continuously below the site at a depth of 8-10 m below ground surface (bgs). This clay layer extends beyond the property boundary in the direction of groundwater flow and separates the aquifer into an upper and lower zone. The TCE contamination plume was caused by TCE DNAPL lenses resting above and below the clay layers (Parker et al., 2008)

The TCE DNAPL source zone was isolated in 2002 using a groundwater extraction, treatment, and re-injection system. The extraction and re-injection system was intended to create a clean water front to flush the downgradient plume. Though the containment system was in operation since 2002, detectable levels of TCE and degradation products still were measured downgradient of the-injection wells. The researchers proposed three hypotheses on why the plume persisted downgradient of the re-injection wells. The first hypothesis was incomplete source-zone capture. The second hypothesis was the occurrence of DNAPL downgradient of the re-injection wells. The third hypothesis was that there was back diffusion from the thin clay layers into the sand aquifer. The first two hypotheses were eliminated, leaving the explanation that back diffusion from the clay layers caused the dissolved TCE plume to persist. To support the hypothesis that back diffusion was the cause of the plume persistence, the researchers used VOC concentration data collected from within and near the clay layers and numerical model simulations (Parker et al., 2008). Their analysis is described in detail, below.

Before source isolation, groundwater sampling was conducted to determine the contaminant distribution downgradient of the source zone. The highest contaminant concentrations occurred close to the clay layers. After the source isolation groundwater

samples were once again collected. The results of those samples showed high contaminant concentrations in the vicinity of the clay layers even after contaminant concentrations would have been expected to decline due to isolation of the source. Core samples collected indicated VOC mass storage in the clay layers.

Using numerical modeling, simulations were run to show if back diffusion is capable of producing the observed field results (Parker et al., 2008). The numerical modeling was conducted using HydroGeoSphere. Simulations were run with a single suspended clay layer in the sand aquifer and with several thin, discontinuous clay layers along with an underlying aquitard. For the case of the single suspended clay layer the model was 2-D with uniform flow occurring in two aquifers separated by a 0.2 m thick clay layer. The contaminant source was a thin TCE DNAPL layer along the top of the clay near the upgradient end of the model domain. The concentration of the TCE in the water adjacent to contaminant source was the TCE solubility limit and the source was assumed to have accumulated over a 35-year period. After the 35-year period, the source concentration was set to zero which allowed for clean water to flush through the system. This simulation was intended to isolate the back diffusion effects from a single clay layer. The results of the simulation showed that 50 years after the source is removed the plume still lingered (Parker et al., 2008).

A simulation was also run where the aquifer contained several suspended, thin, discontinuous clay layers along with an underlying clay aquitard. The thickness of these clay layers was 0.4 m to 0.6 m. For a 30-year period, a constant concentration of TCE at its solubility limit was placed on top of the clay layers. At the end of the 30-year period, the source was removed and the aquifer was flushed with clean water for 200 years. The

plume still persisted 50 years after the source was removed. After 200 years, concentrations at some locations in the model dropped to below 0.01 mg/L except in the vicinity of "one thicker clay layer" (Parker et al., 2008). In the vicinity of the clay aquitard at the bottom of the aquifer, higher contaminant concentrations still persisted. It was noted that diffusion out of the clay aquitard was what contributed to these higher concentrations. Parker et al. (2008) concluded that the stored mass in the clay aquitard was released more slowly as compared to the release from the suspended clay layers because only the top surface of the clay aquitard is flushed and the contaminant diffused deeper into the clay aquitard compared to the suspended clay layers.

Sale et al. (2008) studied the effect that back diffusion from low permeability layers had on downgradient water quality. A two-layer system consisting of a transmissive sand layer and a low permeability silt layer was studied. In the transmissive layer, a high concentration source analogous to a thin DNAPL pool was introduced above the low permeability layer. The source's dissolved constituents were transported in the transmissive zone by advection and by transverse diffusion in the low permeability layer. After the source was removed, the concentration gradient between the low permeability layer and the transmissive layer was reversed causing back diffusion of the contaminants from the low permeability layer into the transmissive layer. This back diffusion can lead to a sustained contaminant concentration in the transmissive layer after the removal of the contaminant source. The authors noted that back diffusion occurs over an even longer time scale than the initial diffusion into the clay layer, with important implications regarding site remediation (Sale et al., 2008).

2.4 DNAPL - Low Permeability Material Interaction

DNAPL in contact with low permeability layer material may alter and modify the material's physical properties, hence allowing enhanced dissolved phase CAH transport into the low permeability layers. Brown and Thomas (1987) studied the mechanism by which low dielectric constant (E) organic chemicals increase the hydraulic conductivity of compacted clay materials. Hydraulic conductivity measurements, basal spacing, electrophoretic mobility, zeta potential, flocculation, and volume change were measured for clay minerals, kaolinite, illite, and smectite (Brown and Thomas, 1987). Since the focus of this current research is on the interaction between DNAPLs and low permeability clay materials, the results of the measurements of hydraulic conductivity, basal spacing and volume change that Brown and Thomas (1987) discuss will be presented in this section.

The hydraulic conductivity measurements were made by compacting mixtures of kaolinite and water, illite and water and smectite and water in 10-cm diameter fixed wall permeameters. Replicates of each mixture were exposed to solutions of "0, 60, 80, and 100% (by volume) ethanol in distilled deionized water; 0, 60, 80, and 100% (by volume) acetone in distilled deionized water; and 0.10, 0.20, and 0.30 M NaCl" (Brown and Thomas, 1987). Results showed that for E values $\leq$40, the hydraulic conductivity increased for kaolinite permeated by acetone. When permeated with ethanol the kaolinite hydraulic conductivity increased when the solution's E value was $\leq$45. Both the acetone and ethanol solutions increased the illite hydraulic conductivity when the solution's E value was less than 45. A decreasing E value corresponds to an increasing organic fraction and a decreasing water fraction of a solution (Brown and Thomas, 1987).

Measurements of smectite clay basal spacing versus mixtures of acetone and ethanol with varying E values were made using x-ray diffraction. Basal spacing is a measurement of space between adjacent layers in a crystalline structure. In general, as basal spacing increases, hydraulic conductivity decreases. According to Brown and Thomas (1987) measurements of basal spacing were only made for smectite clay because only smectite clay undergoes changes in basal spacing when permeated by concentrated organic liquids. The basal spacing for smectite equilibrated with water was 1.8 nm. Dilute concentrations of acetone (2-5%) with E values of 77 and 76, respectively, caused the basal d spacing of the smectite to increase to 2.0 nm. An acetone in water E value of 49 caused the basal d spacing to decrease to 1.8 nm. The basal spacing decreased to 1.4 nm when the solutions E value was decreased to 43 (Brown and Thomas, 1987).

In dilute ethanol solutions the smectite basal spacing increased to 2.3 nm. For a solution E value of 57 the spacing decreased to 2.0 nm. For solution E values below 35 the spacing decreased to 1.6 nm (Brown and Thomas, 1987).

The results of the measurements showed that dilute concentrations of organic liquids increase the basal spacing of the clay material which in turn decreases the hydraulic conductivity of the clay material (Brown and Thomas, 1987).

Finally Brown and Thomas (1987) measured the volume changes of the clay materials when exposed to acetone, xylene, and water. Their results showed that xylene (E=2.4) caused the materials to swell the least and water (E=78) caused the materials to swell the most. The smectite material swelled the most, which the authors attributed to the increased basal spacing. Changes in the particle spacing are what caused the kaolinite and illite to swell (Brown and Thomas, 1987).

Brown and Thomas (1987) came to the conclusion that as organic liquids displace water that is in equilibrium with clay soil, the soil will shrink, causing cracks to form which can act as channels for liquids to flow. This results in an increase in hydraulic conductivity.

Clay-DNAPL interaction may not be the only cause of crack formation in clay. Fookes and Denness (1969) theorized the natural existence of cracks in clay. The research performed by Fookes and Denness (1969) was conducted to determine the fissure patterns in soft rocks so that the engineering behavior of fissured sediments could be analyzed. The fissure patterns of Chalk, Gault, and Weald Clays were examined and it was concluded that differences between fissure patterns could be explained by considering the geology of where the materials came from.

This current research is intended to develop a better understanding of the impact that pooled DNAPLs have on low permeability clay layers and understand how the transport and storage of dissolved CAHs are affected by this impact, or alternatively, affected by the natural presence of cracks in the clay matrix. Brown and Thomas (1987) showed that organic liquids can increase the hydraulic conductivity of clay materials by shrinking the clay, which allows cracks to develop, thereby allowing organic liquids to move more freely into the clay material. Fookes and Denness (1969) showed that cracking is commonly found in clays. The next section is intended to establish the framework for how modeling can be used to simulate the transport of dissolved CAHs within the cracks of low permeability clay layers.

2.5 Modeling Contaminant Transport in Cracks

Grisak and Pickens (1980) used numerical modeling to describe solute transport through fractured media that accounted for the effect of matrix diffusion on transport. Their conceptual model included mobile water in highly permeable fractures and immobile water in a low permeability matrix. Their model accounted for the following: 1) diffusion of solute from the fractures into the low permeability matrix; 2) advection and dispersion due to water flow in the fractures; and 3) linear, equilibrium sorption in the matrix.

The dominant transport mechanism in a fracture is advection-dispersion, while in the unfractured matrix, the dominant transport mechanism is Fickian diffusion. Matrix diffusion is considered a much slower transport process than the advection-dispersion transport process. Figure 2 shows solute transport in a single fracture surrounded by an unfractured matrix. The input concentration of the solute is C_o and the fracture aperture width is 2b. The solute is being transported down the fracture by advection/dispersion and transported into the surrounding matrix by diffusion. The solute profile in the fracture and the matrix is depicted by the hatched area of the figure. There is a zero concentration gradient ($\partial C/\partial y=0$) at the center of each matrix block, which assumes that there are other fractures at a distance 2B from the center of the fracture being simulated.

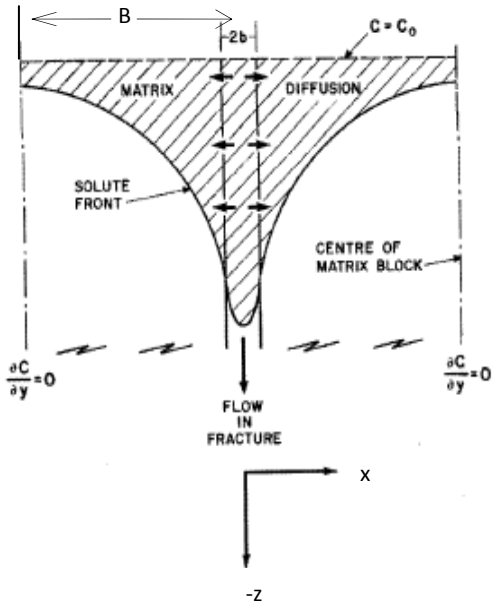

Figure 2: Solute Transport in a Fracture of aperture 2b (after Grisak and Pickens, 1980)

Grisak and Pickens (1980) conducted sensitivity analyses to determine how various parameter values affected solute transport in a fracture system. To study the effect of diffusion within the matrix, Grisak and Pickens (1980) applied a constant concentration source (concentration = C_0) at z = 0, and plotted relative concentration, C/C_o, versus time breakthrough curves at z = -0.76 m for matrix diffusion coefficients ranging from 0.0 cm^2/s to 10^{-6} cm^2/s. The breakthrough curves indicated that as the diffusion coefficient got larger the effect of matrix diffusion became more pronounced and the shallower the breakthrough curves became. The authors theorized that if the concentration source was cut off, then a concentration gradient between the fracture and the matrix would be established and the solute stored in the matrix would be transported by back diffusion into the fracture (Grisak and Pickens, 1980).

Next the effect of aperture size was considered. Assuming a constant fluid velocity in the fracture, reducing the aperture size reduces the quantity of solute

transported in the fracture and increases the relative amount of solute that enters the matrix, since for a given diffusion coefficient, the mass flux of solute into the matrix is controlled by the concentration gradient only. When the aperture size is decreased the fraction of solute transported in the fracture is decreased while the fraction of solute diffused into the matrix is increased. The results are that a relatively larger mass of solute is retained near the source at z = 0 (Grisak and Pickens, 1980).

To study the effect of fluid velocity in the fracture, the velocity was varied from 1 to 60 m/d with other parameters held constant. The conclusion is that an increase in fluid velocity leads to an increase in the ratio of solute-transported to solute-stored in the matrix (Grisak and Pickens, 1980).

To study the effect of dispersion in the fractures, the longitudinal dispersivity was varied. The results show that the larger the dispersivity, the earlier the breakthrough at y = 0.76 m. With small values of dispersivity, no significant breakthrough occurs because without spreading, there is a large concentration gradient maintained between solute in the fractures and the matrix, and therefore, an increase in solute diffusion into the matrix.

The effect of the matrix porosity was evaluated for various fracture aperture sizes. The matrix porosities were varied and results show that for small matrix porosities and larger aperture sizes the solute concentration more rapidly approaches its maximum breakthrough concentration. This intuitively makes sense, since small matrix porosities result in smaller amounts of solute transported from the fracture into the matrix (Grisak and Pickens, 1980).

The distribution coefficient, K_d, describes linear, equilibrium sorption of solute between sorbed and dissolved phases. Grisak and Pickens (1980) assumed sorption in the

matrix only. Varying the distribution coefficient values, they found that for larger K_d values there were larger net solute fluxes into the matrix from the fracture (Grisak and Pickens, 1980). This is because that the larger the distribution coefficient, the less solute is in the dissolved phase in the matrix, and the higher the concentration gradient between the fractures and matrix.

Kueper and McWhorter (1991) studied the conditions that allow DNAPL to enter an initially water saturated fracture. They considered the height of the DNAPL pool that must accumulate over the fracture before the DNAPL will enter the fracture and used numerical modeling to demonstrate DNAPL transport through fractures. The modeling shows that DNAPL entry pressure, which is determined by the height of the DNAPL pool above the fracture, is inversely proportional to fracture aperture and directly proportional to the interfacial tension between the DNAPL and water in the fracture (Kueper and McWhorter, 1991).

Numerical modeling also indicated that DNAPL transport time through a fractured aquitard is inversely proportional to the DNAPL pool height, the fracture aperture size, and the dip of the fracture measured from the horizontal plane. Downward water gradients across the aquitard increased the DNAPL flux into aquitard fractures and upward water gradients decreased the rate of DNAPL movement downward (Kueper and McWhorter, 1991).

Parker et al. (1994) developed a revised conceptual model of DNAPL fate and transport in fractured clay deposits and sedimentary rock. They recognized the fact that the DNAPL in the fracture can be transformed from the immiscible phase to the dissolved phase, which then can diffuse into the porous matrix and remain in the dissolved phase or

sorb onto the matrix material. In essence, Parker et al. (1994) considered both the dissolved transport represented in the Grisak and Pickens (1980) model, and the separate phase transport simulated by Kueper and McWhorter (1991). Factors identified that affect transport are the physical and chemical properties of the DNAPL and geologic material and the extent to which the DNAPL is replenished from DNAPL pools above the fracture(s) or other DNAPL filled fractures. Moderate to narrow aperture size, high aqueous solubility, large porosity, and high sorption capacity of the matrix were shown to enhance the rate of the immiscible phase loss (Parker et al., 1994).

Other published studies of contaminant transport through a fractured have come up with conclusions similar to the studies that have been discussed. Rowe and Booker (1990) concluded that in a situation where a clay aquitard contains fractures and is located above an aquifer, water quality degradation in the aquifer could be significant as a result of contaminant transport down through the aquitard fractures and into the aquifer. Harrison et al. (1992) used modeling to show that vertical fractures that fully penetrate an aquitard and have fracture aperture sizes of at least 10 μm can provide an advective transport pathway for dissolved contaminants that can lead to considerable degradation of water quality if an aquifer is present below the aquitard (Harrison et al., 1992). Reynolds and Kueper (2002) concluded that the fracture aperture is the most important factor controlling DNAPL migration through a fracture. By increasing the fracture aperture from 15 μm to 50 μm there was a 20 fold increase in the rate of DNAPL migration downward (Reynolds and Kueper, 2002). They further concluded that DNAPL migration rates are not significantly influenced by varying the parameters governing matrix diffusion.

Models such as the one presented by Grisak and Pickens (1980) may be useful in simulating dissolved solute transport into and out of low permeability clay materials that contain fractures, referred to as cracks from this point on. This research assumes that the interaction between the DNAPL and the low permeability clay causes the cracks to form in the clay, or alternatively, that cracks pre-existed in the clay. The DNAPL dissolves, and the dissolved CAH is transported by advection into the cracks. From the cracks, the dissolved CAH diffuses into the surrounding clay matrix. The dissolved phase is also transported in the aquifer by advection/dispersion downgradient of the DNAPL source. Chapter 3 will discuss the methodology used to model these coupled transport processes in order to quantify the impact that enhanced transport into and out of low permeability layers has on dissolved CAH plume evolution and longevity.

3.0 Methodology

3.1 Overview

In this chapter, the approach taken to model the enhanced transport of dissolved CAH into and out of a low permeability clay layer due to a DNAPL pool sitting atop the layer will be presented. The model is demonstrated using the physical and chemical properties of a common CAH of particular importance to the DoD, TCE. The conceptual model consists of a high conductivity sand layer on top of a low conductivity clay layer (see Figure 3). Cracks are hypothesized to exist in the low conductivity clay, either due to clay-DNAPL interaction or the natural existence of cracks in the clay (Fookes and Denness, 1969). We may model the cracks in the clay as regions of mobile water, while the surrounding non-cracked clay matrix may be represented as an immobile region. As the cracks form, the mobile porosity of the clay increases as the immobile porosity decreases. In this study, model simulations are run to simulate the effect of cracking in the clay layer on dissolved contaminant transport. We hypothesize that "enhanced diffusion" due to the cracks in the clay, which permits contaminant advection through the cracks in addition to diffusion in the clay itself, may significantly affect overall contaminant transport.

3.2 General Model Description

The key assumption of this research is that low permeability layers contain cracks, either naturally occurring or the result of DNAPL pooling on top of the layer. Upon the formation of the cracks, the pooled DNAPL dissolves, and the dissolved CAH is then transported into the cracks by advection and dispersion. From the cracks, the

CAH diffuses into the surrounding low permeability layer. As stated above, this transport by advection/dispersion into the cracks and diffusion from the cracks into the surrounding low permeability layer results in "enhanced diffusion." The assumption is that this enhanced diffusion process leads to increased storage of CAH as compared to the CAH storage that would result from transport by only Fickian diffusion within the intact low permeability layer.

Figure 3 depicts a general conceptual model for this research. A pool of DNAPL collects on the surface of cracked low permeability clay. From the DNAPL pool aqueous phase CAH is transported into the cracks by advection/dispersion and from the cracks mass is transferred to the immobile region of the low permeability clay by diffusion. Aqueous phase CAH is also transported downgradient in the sand layer by advection, dispersion, and linear, equilibrium, sorption.

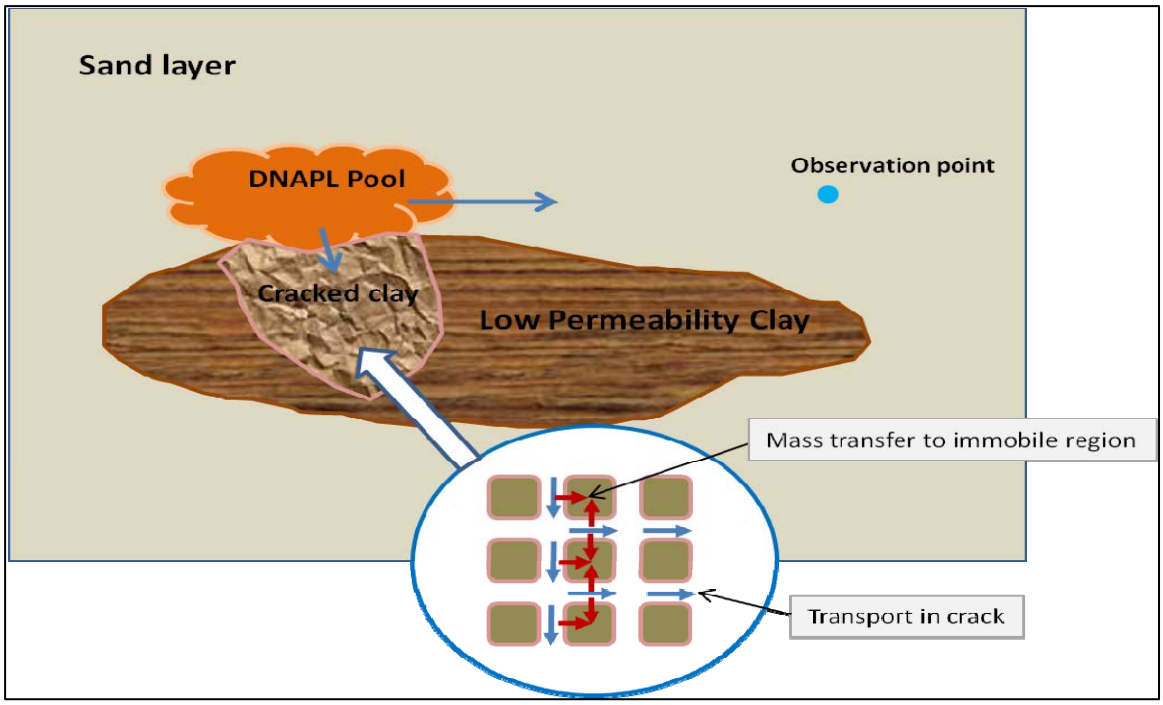

Figure 3: Research Conceptual Model Depicting Advective/Dispersive Transport in Crack, and Mass Transfer to Immobile Region by Diffusion (represented as first order mass transfer process)

Figure 4 depicts a simplified conceptual model that we can use to study the impact of enhanced diffusion on contaminant transport. In essence, the scenario depicted in Figure 4 couples the conventional model of advective-dispersive-sorptive transport in a high conductivity sand layer with the Grisak and Pickens (1980) model of advective/dispersive transport in fractures and diffusive transport in the surrounding unfractured low conductivity matrix. In Figure 4, dissolved CAH from the DNAPL pool is assumed to move into cylindrical cracks of radius b by advection and then diffuse from the cracks into the low permeability layer. Dissolved CAH also diffuses directly into the low permeability layer from the DNAPL pool. In the high conductivity sand, dissolved CAH is transported downgradient in the x-direction by advection and dispersion. This model assumes that a linear, reversible, equilibrium relationship describes sorption of dissolved CAH onto both the sand and clay (both at the cracks and within the clay

matrix), but the extent of sorption on sand is much less than the extent of sorption on clay.

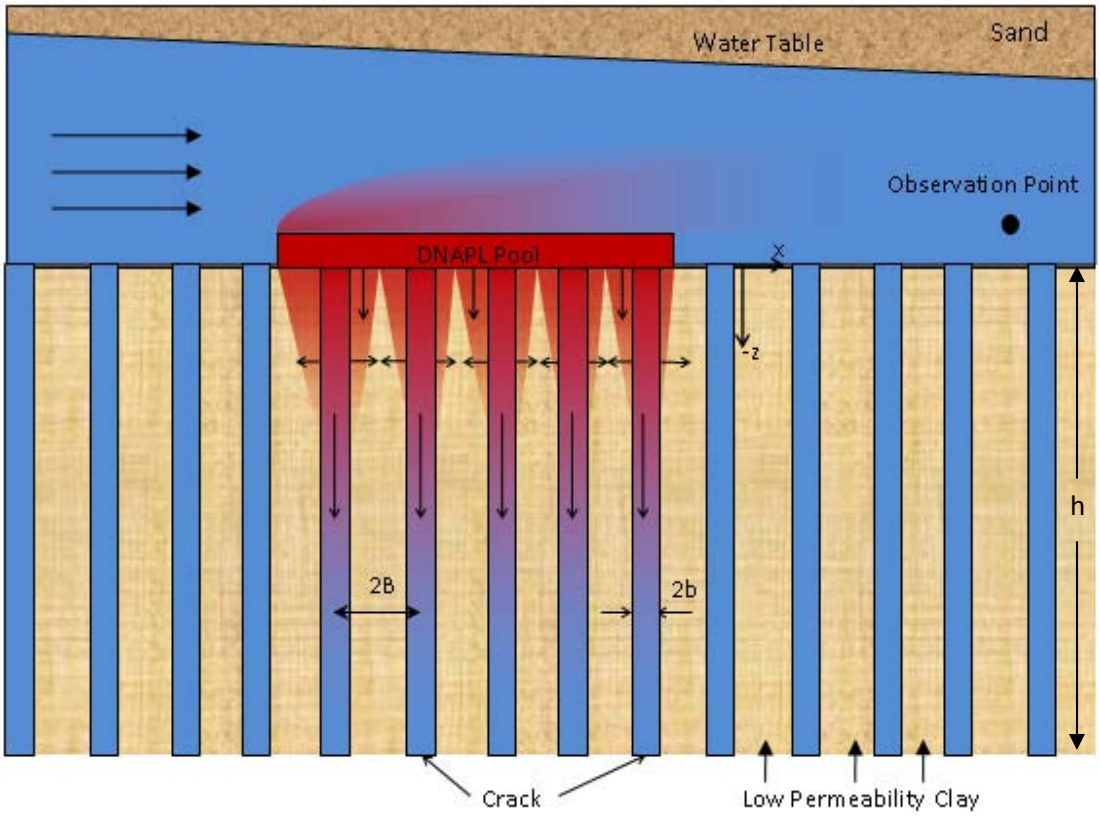

Figure 4: Low Permeability Layer with Cracks Formed by Pooled DNAPL Below a High Permeability Sand Aquifer

3.3 Model Equations

Equation 3.1 (Zheng and Wang, 1999) is the governing equation that describes contaminant fate and transport in the sand aquifer layer above the low permeability clay.

$$R\theta \frac{\partial C}{\partial t} = \frac{\partial}{\partial x_i}\left(\theta D_{ij}^{s} \frac{\partial C}{\partial x_j}\right) - \frac{\partial}{\partial x_i}(\theta v_i^{s} C) \qquad \text{(Eq 3.1)}$$

where R [-] is the retardation factor for the sand aquifer layer, θ [-] is the porosity of the sand, C [ML^{-3}] is the concentration of dissolved CAH in the sand aquifer layer, t [T] is time, x [L] is the distance along the respective Cartesian coordinate axis, D_{ij}^{s} [L^2T^{-1}] is the

hydrodynamic dispersion coefficient tensor for sand, and v_i^s [LT^{-1}] is the linear pore water velocity. The dispersion coefficients are related to the water velocity by Equations 3.2 and 3.3.

$$D_L = \alpha_L v_i \quad \text{(Eq 3.2)}$$

and

$$D_T = \alpha_T v_i \quad \text{(Eq 3.3)}$$

where D_L [L^2T^{-1}] is the longitudinal dispersion coefficient, D_T [L^2T^{-1}] is the transverse dispersion coefficient, α_L [L] is the longitudinal dispersivity, and α_T is the transverse dispersivity. Note that D_L is D_{ij}^s when i = j = x, and x is the direction of flow, and D_T is D_{ij}^s when i = j = y and y is the direction transverse to the flow direction.

In Equation 3.1, advection in the sand layer is represented by $\frac{\partial}{\partial x_i}(\theta v_i C)$, and dispersion is represented by $\frac{\partial}{\partial x_i}\left(\theta D_{ij}^s \frac{\partial C}{\partial x_j}\right)$. Equation 3.4 relates the sorbed concentration to the concentration of dissolved CAH (C) by a linear, reversible, equilibrium isotherm:

$$\bar{C} = K_d^s C \quad \text{(Eq 3.4)}$$

where $\bar{C}$ [MM^{-1}] is the concentration of contaminant sorbed to sand. The retardation factor (R) in Equation 3.1 is defined as:

$$R = 1 + \frac{\rho_b^s}{\theta}\frac{\partial \bar{C}}{\partial C} = 1 + \frac{\rho_b^s}{\theta}K_d^s \quad \text{(Eq 3.5)}$$

where, ρ_b^s[ML^{-1}] is the bulk density of sand, and K_d^s [L^3M^{-1}] is the sorption distribution constant for sand.

Darcy's Law, represented by Equation 3.6 couples the hydraulic conductivity and gradient to the advective velocity term.

$$v_i = \frac{q_i}{\theta} = -\frac{K_i}{\theta}\frac{\partial h}{\partial x_i} \quad \text{(Eq 3.6)}$$

where q_i [$L^3L^{-2}T^{-1}$] is the volumetric flow rate per unit surface area of aquifer (also referred to as the Darcy velocity), K_i [LT^{-1}] is the principal component of the sand hydraulic conductivity tensor, and h [L] is the hydraulic head in the sand aquifer.

Equation 3.7 is Equation 3.1 with the addition of a source/sink term.

$$R\theta\frac{\partial C}{\partial t} = \frac{\partial}{\partial x_i}\left(\theta D_{ij}^s\frac{\partial C}{\partial x_j}\right) - \frac{\partial}{\partial x_i}(\theta v_i C) \pm q_s C \quad \text{(Eq 3.7)}$$

where q_s [T^{-1}] is the volumetric flow rate per unit volume of aquifer representing fluid sources (positive) and sinks (negative).

As shown in Figure 4, below the sand aquifer is a low permeability clay layer that contains cracks caused by pooled DNAPL. To model this situation a dual porosity, or dual domain, model is used. A dual domain model is ideal for modeling contaminant transport in fractured media. In a dual domain model, water is assumed to be either mobile or immobile. Contaminant can be transported by advection, dispersion, and sorption in the mobile water, while in the immobile water, there is no contaminant transport, though equilibrium sorption may be modeled using an immobile domain retardation factor. Exchange of contaminant between the mobile and the immobile domains is assumed to be governed by a first-order rate process, characterized by a first-order rate constant (Zheng and Wang, 1999).

The governing equations adapted from Zheng and Wang (1999) for a dual domain system with sorption are:

$$\theta_m R_m\frac{\partial C_m}{\partial t} + \theta_{im} R_{im}\frac{\partial C_{im}}{\partial t} = \frac{\partial}{\partial x_i}\left(\theta_m D_{ij}^c\frac{\partial C_m}{\partial x_j}\right) - \frac{\partial}{\partial x_i}(\theta_m v_i^c C_m) \quad \text{(Eq 3.8)}$$

and

$$\theta_{im} R_{im} \frac{\partial C_{im}}{\partial t} = \xi(C_m - C_{im}) \quad \text{(Eq 3.9)}$$

where C_m [ML^{-3}] is the concentration of dissolved CAH in the mobile domain, C_{im} [ML^{-3}] is the concentration of dissolved CAH in the immobile domain, R_m [-] is the retardation factor for the mobile domain, R_{im} [-] is the retardation factor for the immobile domain, θ_m [-] is the porosity of the mobile domain, defined as volume of mobile water per total volume of the medium, θ_{im} [-]is the porosity of the immobile domain, defined as volume of immobile water per total volume of the medium. When z=0 in Figure 4 C_m and C_{im} equal C in Equation 3.7. D_{ij}^c is the dispersion coefficient of the dissolved CAH in the cracks, v_i^c is the pore water velocity in the cracks, and ζ [T^{-1}] is the first order mass transfer rate between the mobile and immobile domains. The equation for R_m is:

$$R_m = 1 + \frac{f\rho_b^c K_d^c}{\theta_m} \quad \text{(Eq 3.10)}$$

where f [-] is the fraction of sorption sites that are in contact with the mobile liquid phase and is approximated by $\frac{\theta_m}{\theta}$, ρ_b^c is the bulk density of the cracked clay, and K_d^c [L^3M^{-1}] is the sorption constant for clay. The equation for R_{im} is:

$$R_{im} = 1 + \frac{(1-f)\rho_b^c K_d^c}{\theta_{im}} \quad \text{(Eq 3.11)}$$

The source/sink term, which is the last term on the right-hand side of Equation 3.7, is used to couple transport in the sand with Equations 3.8 and 3.9 describing transport in the cracked clay. The model developed for this research assumes that no biological or chemical degradation of the contaminant occurs.

3.4 Model Implementation in GMS

Using DoD's Groundwater Modeling System (GMS) "enhanced diffusion" of dissolved phase CAH into low permeability clay from a pool of DNAPL and back diffusion of dissolved phase CAH out of the low permeability clay is modeled. GMS uses MODFLOW to generate the model's groundwater flow contours. MODFLOW determines these contours by first generating a steady-state potential field based on boundary conditions and the main equation of flow. Then, using Equation 3.6, with the specified hydraulic conductivities, MODFLOW determines steady groundwater velocities throughout the model domain. The velocity field is then used in Equation 3.7 or 3.8 (depending on whether a single or dual domain transport model is being formulated). Equation 3.7 or 3.8 is simulated by Modular Three-Dimensional Multispecies Transport Model Multi-Species (MT3DMS) to simulate advection/dispersion, sorption, diffusion and biological or chemical reactions of dissolved contaminants in groundwater.

Within GMS, a 100 m long by 70 m wide by 6 m deep sand aquifer was constructed above a 100 m long by 12 m deep by 30 m wide low conductivity clay layer. In MODFLOW values of the vertical and horizontal hydraulic conductivity, longitudinal dispersivity and mobile porosity were assigned to the sand and clay. Also to establish a hydraulic gradient in the model, the heads on the left and right side of the model were 20.5 m and 19.5 m, respectively. Using MT3DMS, the advection, dispersion, sorption, and diffusion transport mechanisms in the sand, and clay are simulated. The simulation consisted of two stress periods. During the first stress period of 10 years, a constant concentration source of 110 mg/L of TCE was introduced just above a 192 m^2 area of the clay. The second stress period was 20 years long during which no additional TCE is

introduced. MT3DMS uses a third-order TVD (ULTIMATE) scheme to solve the advection piece of the model. The ratio of horizontal transverse dispersivity to longitudinal dispersivity is 0.1 and the ratio of vertical transverse dispersivity to longitudinal dispersivity is 0.01. An effective molecular diffusion coefficient of 8.64 x 10^{-6} L^2-T^{-1} is assigned to the sand and clay. Dual-domain mass transfer (with sorption) was assumed for every model run except Scenario 1 mentioned below. TCE concentration versus time data were calculated at a single observation point 56 m downgradient from the center of the TCE source.

Figure 5 is a conceptual depiction of the GMS model. The non-aqueous phase TCE Source (DNAPL Pool) is transformed into aqueous phase TCE and is transported into the mobile domain (crack) and downgradient in the high permeability layer (sand layer) by advection/dispersion. The TCE source is represented in GMS as constant concentration cells, which are set to zero when the source is removed. Diffusion between the mobile domain and the immobile domain (low permeability clay) is modeled as a first-order process characterized by a first order mass transfer rate constant (ζ). Within the mobile and immobile domains the aqueous TCE is assumed to be well mixed. $C_m(z,t)$ and $C_{im}(z,t)$ represent the aqueous TCE concentration at a given point, z, and time, t, in the mobile and immobile domains, respectively. Both the mobile and immobile domains have retardation factors represented by R_m for the mobile domain and R_{im} for the immobile domain. R_m and R_{im} are calculated using Equations 3.10 and 3.11 respectively. K_d represents the ratio of sorbed to dissolved TCE concentrations in the clay.

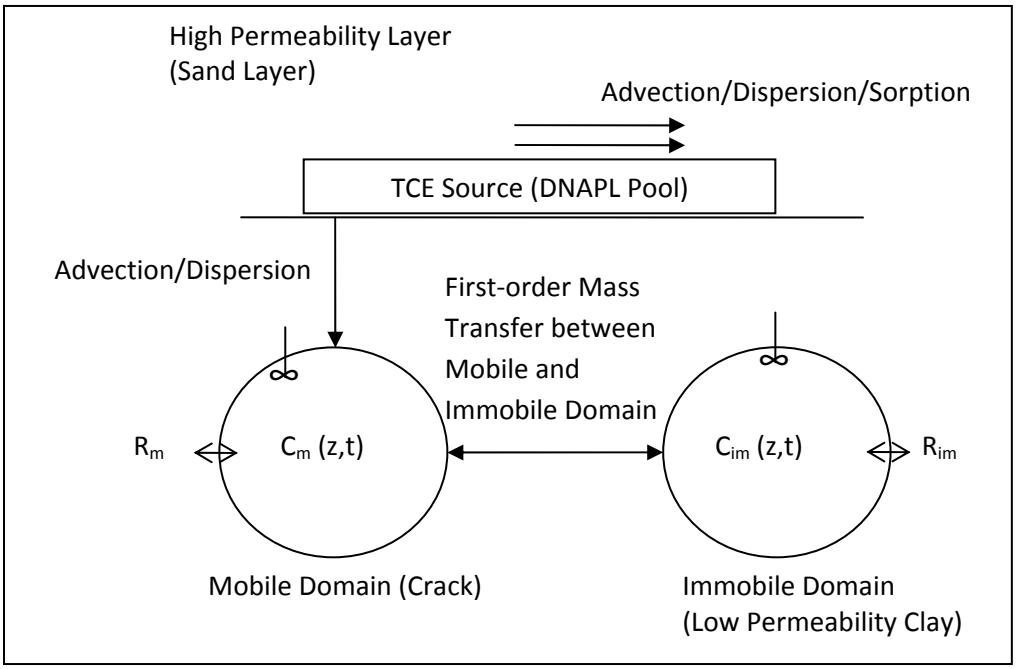

Figure 5: Conceptual Depiction of Dual-Domain GMS Model.

To simulate cracks in the clay, the values of the clay's mobile and immobile porosity were modified in MODFLOW and MT3DMS. To simulate the formation of additional cracks the clay's mobile porosity (θ_m) was increased as the immobile porosity (θ_{im}) decreased. In the absence of cracks, the clay was assumed to have a mobile porosity of zero and an immobile porosity(θ_{im}^0) of 0.43. To calculate the immobile porosity (θ_{im}) of the cracked clay, Equation 3.12 is used.

$$\theta_{im} = \theta_{im}^{o}(1 - \theta_m) \qquad \text{(Eq 3.12)}$$

where θ_m [-] is the mobile porosity assigned in MODFLOW and θ_{im} [-] is assigned in MT3DMS. To determine the total porosity (θ) of cracked clay Equation 3.13 was used.

$$\theta = \theta_m + \theta_{im}^0(1 - \theta_m) = \theta_m + \theta_{im} \qquad \text{(Eq 3.13)}$$

In MT3DMS values of bulk density values were assigned to the sand and clay. The bulk density (ρ_b) was calculated using Equation 3.14.

$$\rho_b = \rho_s(1 - \theta) \quad \text{(Eq 3.14)}$$

where ρ_s [kg-m^{-3}] is the solid density. The value of ρ_s for sand is 2649 kg-m^{-3} and for clay is 2630 kg-m^{-3} (Chapman and Parker, 2005). The θ of the sand, which is set equal to θ_m of the sand since sand is assumed to have no immobile porosity, is 0.35 (Chapman and Parker, 2005). Thus, the sand ρ_b value used in every model run is 1722 kg-m^{-3}. The value of ρ_b assigned to the clay varied from model run to model run because the value of ρ_b depends on the value of θ, per Equation 3.14, and the value of θ varies with the value of θ_m assigned to the clay, per Equation 3.13.

To solve for B in Figure 4 Equation 3.15 is used (Goltz and Roberts, 1988).

$$\frac{\xi}{\theta_{im} R_{im}} = \frac{3D_{eff}}{B^2 R_{im}} \quad \text{(Eq 3.15)}$$

where B [L] is the half-distance between cracks as depicted in Figure 4, ζ [T^{-1}] is the rate constant for mass transfer between the low permeability clay and the crack, θ_{im} [-] is the porosity of the low permeability clay, R_{im} [-] is the retardation factor of the low permeability clay, and D_{eff} [L^{2}T^{-1}] is the effective diffusion coefficient within the clay calculated using Equation 2.2.

To solve for the radius, b, of a single crack the total volume of cracks must first be determined. Equation 3.16 is used to determine the total volume of cracks which is represented by the volume of mobile void space.

$$\theta_m = \frac{\text{volume mobile void space}}{\text{Total Volume}} \quad \text{(Eq 3.16)}$$

where θ_m [-] is the porosity of the mobile void space in the low permeability layer. The cracks in the low permeability clay represent the mobile void space. With the total

volume of cracks determined, Equation 3.17 can be used to determine the radius, b of a single crack.

$$\text{Volume Mobile Void Space} = c\pi b^2 h \qquad \text{(Eq 3.17)}$$

where c [-] is the number of cracks in the clay, b [L] is the radius of a single crack, and h [L] is the height of the crack (see Figure 4). The number of cracks in the clay, needed to apply Equation 3.17, is determined using Equation 3.18.

$$c = \left(\frac{L}{2B} + 1\right)\left(\frac{W}{2B} + 1\right) \qquad \text{(Eq 3.18)}$$

where L [L] is the length and W [L] is the width of the cracked clay region.

Table 1 lists the crack radius (b) as depicted in Figure 4, and the half distance between cracks (B) calculated using Equations 3.15 through 3.18 based on the value of θ_m.

Table 1: Crack Radius, Half Distance Between Cracks and Total Number Cracks Based On θ_m

θ_m (-)	c (-)	b (m)	B (m)
0.001	0	0	0
0.01	341,239	0.005	0.047
0.1	375,292	0.016	0.045
0.5	674,859	0.027	0.033

3.5 Model Scenarios

Two initial model scenarios were considered. Scenario 1 was a high permeability sand that contained a TCE source. Table 2 lists the MODFLOW parameters used and Table 3 lists the MT3DMS parameters used. Due to the fact that there was no clay in this scenario the model was run without immobile porosity or first order mass transfer rate constant.

Table 2: Scenario 1 MODFLOW Material Property Input Parameters

Material	Horizontal K_h (m/d)	Vertical K_v (m/d)	Longitudinal Dispersivity (m)	Mobile Porosity (θ_m)
Sand[(1)]	17.28	1.728	1.0	0.35
Clay	N/A	N/A	N/A	N/A

[(1)] (Chapman and Parker, 2005)

Table 3: Scenario 1 MT3DMS Input Parameters

Material	Bulk Density (ρ_b) (kg-m^{-3})	Immobile Porosity (θ_{im})	Sorption Constant (K_d) (m^3-kg^{-1})	First Order Mass Transfer Rate Constant (ζ) (d^{-1})
Sand	1722	N/A	0.00017[(1)]	N/A
Clay	N/A	N/A	N/A	N/A

[(1)](Sale et al., 2008)

Scenario 2 was high permeability sand located above a low permeability clay layer that was free of cracks. On the surface of the low permeability clay layer was a pool of TCE. Table 4 lists the MODFLOW parameters used and Table 5 lists the MT3DMS parameters used. As mentioned earlier this research assumed that uncracked clay has no mobile porosity. To simulate this, a value of 0.001 was assigned for the mobile porosity of the clay (see Table 4). Recall the clay total porosity is 0.43; thus, an immobile porosity of 0.429 was assumed for the uncracked clay (see Table 5).

Table 4: Scenario 2 MODFLOW Material Property Input Parameters

Material	Horizontal K_h (m/d)	Vertical K_v (m/d)	Longitudinal Dispersivity (m)	Mobile Porosity (θ_m)
Sand[(1)]	17.28	1.728	1.0	0.35
Clay	4.32E-5[(1)]	4.32E-6[(1)]	1.0E-4	0.001

[(1)] (Chapman and Parker, 2005)

Table 5: Scenario 2 MT3DMS Input Parameters

Material	Bulk Density (ρ_b) (kg-m^{-3})	Immobile Porosity (θ_{im})	Sorption Constant (K_d) (m^3-kg^{-1})	First Order Mass Transfer Rate Constant (ζ) (d^{-1})
Sand	1722	0.00001	0.00017[(1)]	0.0
Clay	1499	0.429	0.051	0.005

[(1)](Sale et al., 2008)

The concentration versus time breakthrough curves generated for Scenarios 1 and 2 are used as "benchmarks" for the parameter sensitivity analysis discussed later.

Scenario 3 was the same as Scenario 2 except Scenario 3 made the assumption that vertical cracks existed in the clay. Values of K_d, ζ, and θ_m used in Scenario 3 are baseline values for the sensitivity analysis to be discussed later. Table 6 lists the MODFLOW parameter values used and Table 7 lists the MT3DMS parameter values used.

Table 6: Scenario 3 MODFLOW Material Property Input Parameters

Material	Horizontal K_h (m/d)	Vertical K_v (m/d)	Longitudinal Dispersivity (m)	Mobile Porosity (θ_m)
Sand[(1)]	17.28	1.728	1.0	0.35
Clay	4.32E-5[(1)]	4.32E-6[(1)]	1.0E-4	0.1

[(1)] (Chapman and Parker, 2005)

Table 7: Scenario 3 MT3DMS Input Parameters

Material	Bulk Density (ρ_b) (kg-m^{-3})	Immobile Porosity (θ_{im})	Sorption Constant (K_d) (m^3-kg^{-1})	First Order Mass Transfer Rate Constant (ζ) (d^{-1})
Sand	1722	0.00001	0.00017[(1)]	0.0
Clay	1349	0.387	0.051	0.005

[(1)](Sale et al., 2008)

3.6 Sensitivity Analysis

A sensitivity analysis was conducted to investigate how varying the sorption distribution coefficient (K_d), mobile porosity (θ_m), and the first order mass transfer rate constant (ζ) affected the downgradient concentration versus time breakthrough curves. The sensitivity analysis conducted for K_d was performed done using values of 0.0051 m^3-kg^{-1}, and 0.51 m^3-kg^{-1}. The breakthrough curves generated are compared to the breakthrough curves for Scenarios 1-3. Table 8 lists the MODFLOW parameters used and Table 9 lists the MT3DMS parameters used.

Table 8: K_d Sensitivity Analysis MODFLOW Material Property Input Parameters

Material	Horizontal K_h (m/d)	Vertical K_v (m/d)	Longitudinal Dispersivity (m)	Mobile Porosity (θ_m)
Sand[(1)]	17.28	1.728	1.0	0.35
Clay	4.32E-5[(1)]	4.32E-6[(1)]	1.0E-4	0.1

[(1)] (Chapman and Parker, 2005)

Table 9: K_d Sensitivity Analysis MT3DMS Input Parameters

Material	Bulk Density (ρ_b) ($kg\text{-}m^{-3}$)	Immobile Porosity (θ_{im})	Sorption Constant (K_d) ($m^3\text{-}kg^{-1}$)	First Order Mass Transfer Rate Constant (ζ) (d^{-1})
Sand	1722	0.00001	0.00017[(1)]	0.0
Clay	1349	0.387	0.0051	0.005
			0.51	

[(1)](Sale et al., 2008)

The sensitivity analysis for θ_m was done using θ_m values of 0.01, and 0.5. The breakthrough curves generated were compared to the breakthrough curves for Scenarios 1-3. Table 10 lists the MODFLOW parameter values used and Table 11 lists the MT3DMS values used. For each θ_m value in Table 9 Equation 13.11 was used to

calculate θ_{im} and Equation 13.13 was used to calculate the corresponding ρ_b value in Table 11.

Table 10: θ_m Sensitivity Analysis MODFLOW Material Property Input Parameters

Material	Horizontal K_h (m/d)	Vertical K_v (m/d)	Longitudinal Dispersivity (m)	Mobile Porosity (θ_m)
Sand[(1)]	17.28	1.728	1.0	0.35
Clay	4.32E-5[(1)]	4.32E-6[(1)]	1.0E-4	0.01
				0.1
				0.5

[(1)] (Chapman and Parker, 2005)

Table 11: θ_m Sensitivity Analysis MT3DMS Input Parameters

Material	Bulk Density (ρ_b) (kg-m^{-3})	Immobile Porosity (θ_{im})	Sorption Constant (K_d) (m^3-kg^{-1})	First Order Mass Transfer Rate Constant (ζ) (d^{-1})
Sand	1722	0.00001	0.00017[(1)]	0.0
Clay	1484	0.4257	0.051	0.005
	750	0.215		

[(1)](Sale et al., 2008)

The final sensitivity analysis conducted was for ζ values of 0.01 d^{-1}, and 0.5 d^{-1}. The breakthrough curves generated are compared to the breakthrough curve for Scenarios 1-3. Table 12 lists the MODFLOW parameters used and Table 13 lists the MT3DMS parameters used.

Table 12: ζ Sensitivity Analysis MODFLOW Material Property Input Parameters

Material	Horizontal K_h (m/d)	Vertical K_v (m/d)	Longitudinal Dispersivity (m)	Mobile Porosity (θ_m)
Sand[(1)]	17.28	1.728	1.0	0.35
Clay	4.32E-5[(1)]	4.32E-6[(1)]	1.0E-4	0.1

[(1)] (Chapman and Parker, 2005)

Table 13: ζ Sensitivity Analysis MT3DMS Input Parameters

Material	Bulk Density (ρ_b) (kg-m^{-3})	Immobile Porosity (θ_{im})	Sorption Constant (K_d) (m^3-kg^{-1})	First Order Mass Transfer Rate Constant (ζ) (d^{-1})
Sand	1722	0.00001	0.00017[(1)]	0.0
Clay	1349	0.387	0.051	0.01
				0.5

[(1)](Sale et al., 2008)

3.7 First Moment Analysis

Since back diffusion causes breakthrough curve tailing, and an understanding of the extent of tailing is crucial in managing a contaminant plume, an analysis of the breakthrough curve's first moment was conducted for this study. The first moment measures the center of mass of the breakthrough curve. A high value for the first moment indicates a high degree of tailing. In this study, the first moment of breakthrough curves was determined for K_d values of 0.051 m^3-kg^{-1} and 0.102 m^3-kg^{-1}. Table 14 lists the MODFLOW parameters used and Table 15 lists the MT3DMS parameters used. The total model run time was 695 years to accurately capture the first moment of the tailing breakthrough curves. The constant 110 mg-L^{-1} TCE source was removed after 10 years.

Table 14: K_d Moment Analysis MODFLOW Material Property Input Parameters

Material	Horizontal K_h (m/d)	Vertical K_v (m/d)	Longitudinal Dispersivity (m)	Mobile Porosity (θ_m)
Sand[(1)]	17.28	1.728	1.0	0.35
Clay	4.32E-5[(1)]	4.32E-6[(1)]	1.0E-4	0.1

[(1)] (Chapman and Parker, 2005)

Table 15: K_d Moment Analysis MT3DMS Input Parameters

Material	Bulk Density (ρ_b) (kg-m^{-3})	Immobile Porosity (θ_{im})	Sorption Constant (K_d) (m^3-kg^{-1})	First Order Mass Transfer Rate Constant (ζ) (d^{-1})
Sand	1722	0.00001	0.00017[(1)]	0.0
Clay	1349	0.387	0.051	0.005
			0.102	

[(1)](Sale et al., 2008)

To calculate the first moment, the area under the concentration versus time curve was calculated using Equation 3.18.

$$\text{area} = \sum_{i=0}^{i_{max}-1} \left[\frac{c(t_{i+1})+c(t_i)}{2}\right](t_{i+1} - t_i) \qquad \text{(Eq 3.18)}$$

where c(t) [mg-L^{-1}] is the concentration output from GMS and t_i [T] is the time.

Then the discrete residence time density function ($f(t_i)$) is determined for each discrete concentration value using Equation 3.19.

$$f(t_i) = \frac{c(t_i)}{\text{area}} \qquad \text{(Eq 3.19)}$$

The first moment is then calculated using Equation 3.20.

$$\bar{t}_{RTD} = \sum_{i=0}^{i_{max}-1} \left[\frac{(t_i+t_{i+1})}{2}\right]\left[\frac{f(t_i)+f(t_{i+1})}{2}\right](t_{i+1} - t_i) \qquad \text{(Eq 3.20)}$$

where $\bar{t}_{RTD}$ [T] is the mean residence time or first moment (Clark, 2009).

4.0 Results and Discussion

4.1 Overview

This chapter presents the breakthrough curves for Scenarios 1-3 and the K_d, θ_m, and ζ sensitivity analysis discussed in Chapter 3. The concentration versus time data was calculated at a single observation point 56 m downgradient from the TCE source. Also presented are the results of the first moment analysis conducted for K_d values of 0.051 m^3-kg^{-1} and 0.102 m^3-kg^{-1}.

4.2 Baseline Simulations

Figure 6 is the breakthrough curves for baseline Scenarios 1-3along with the TCE maximum contaminant level (MCL) of 0.005 mg-L^{-1} for comparison.

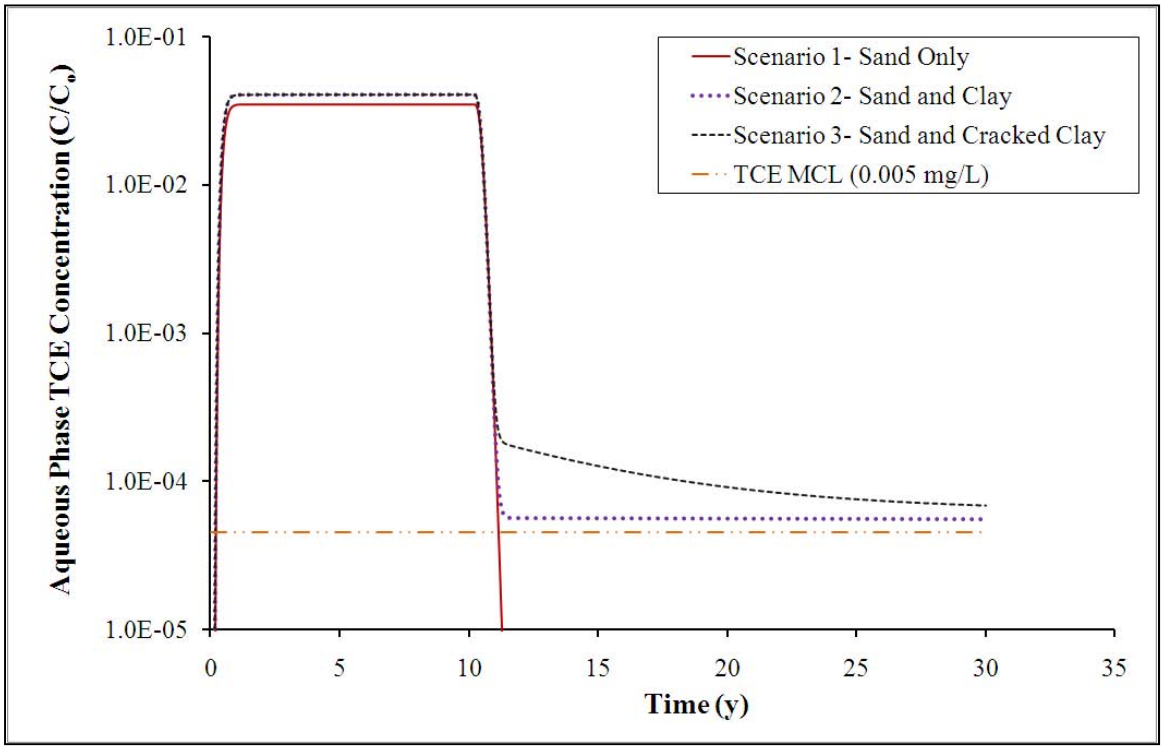

Figure 6: Breakthrough Curves for Scenarios 1-3

These three breakthrough curves will be used to compare to the breakthrough curves for the K_d, θ_m, and ζ sensitivity analysis.

Scenario 1 represents high permeability sand with a constant 110 mg-L^{-1} TCE source that disappears after 10 years. For the remaining 20 years, the sand is flushed with uncontaminated water. The breakthrough curve in Figure 6 indicates that after the TCE source is removed the aqueous phase TCE concentration in the sand rapidly drops and tails off towards zero. The tailing effect is not represented in Figure 6.

Scenario 2 consists of high permeability sand atop an uncracked low permeability clay layer. A 110 mg-L^{-1} TCE source is used to represent a DNAPL pool atop the clay layer. The source remains for 10 years. This scenario assumes that the dominant transport mechanism of the aqueous phase TCE into the clay from the DNAPL pool is Fickian diffusion. The tailing of the breakthrough curve beginning at approximately 11 years for Scenario 2 reflects the "back diffusion" of the aqueous phase TCE from the uncracked clay into the sand aquifer where advection then becomes the dominant transport mechanism. Figure 6 also indicates that the downgradient aqueous phase TCE concentration is still above the U.S. EPA maximum contaminant level (MCL) of 0.005 mg-L^{-1} 20 years after the TCE source is removed.

Scenario 3 is the same as Scenario 2 except Scenario 3 contains cracked clay instead of just clay. The tailing in Scenario 3 is greater than the tailing in Scenario 2, due to enhanced "back diffusion" of aqueous phase TCE from the cracked clay into the sand aquifer. Also, the downgradient TCE concentration is still above the U.S. EPA maximum contaminant level (MCL) of 0.005 mg-L^{-1} 20 years after the TCE source is removed.

Tailing, which is the significant difference between the three breakthrough curves in Scenarios 1 through 3, is due to the low permeability clay in Scenarios 2 and 3. The aqueous phase TCE is "stored" in the clay until the DNAPL source is depleted in the sand aquifer. Upon removal of the DNAPL source, the aqueous phase TCE "stored" in the clay "back diffuses" into the sand, where it is then transported downgradient by advection. This "back diffusion" process results in the breakthrough curve tail for Scenarios 2 and 3. The tailing that occurs in Scenarios 2 and 3 is similar to the tailing observed by Chapman and Parker (2005) in their investigation of back diffusion of TCE from a clayey silt aquitard.

4.3 Sensitivity Analysis

A sensitivity analysis is conducted for K_d, θ_m, and ζ. For each sensitivity analysis, the breakthrough curve is plotted and compared to the breakthrough curves generated for the baseline scenarios. The first sensitivity analysis conducted considers how the results of the model would change if K_d of the clay is changed. The values of K_d considered are 0.0051 m^3-kg^{-1}, and 0.51 m^3-kg^{-1}. Baseline parameter values for θ_m and ζ of 0.1 and 0.005 d^{-1} respectively were used. Figure 7 depicts the breakthrough curves for the two different K_d values along with the breakthrough curves the baseline scenarios.

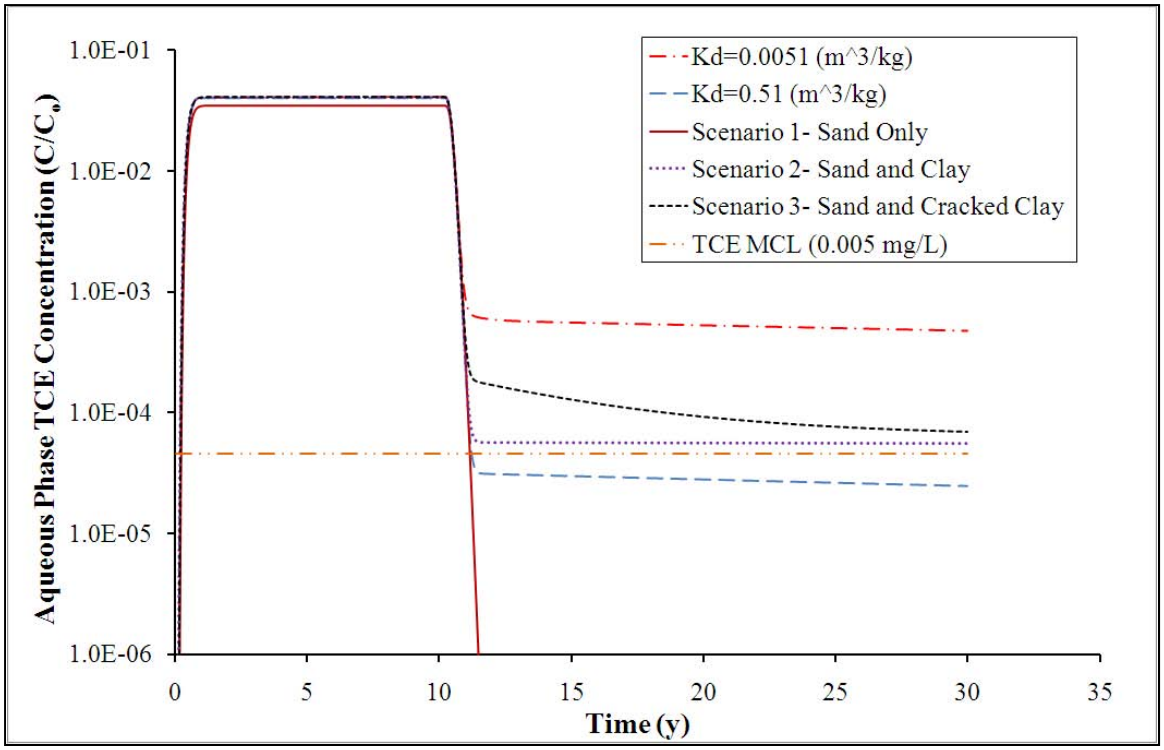

Figure 7: Breakthrough Curves for K_d Sensitivity Analysis along with Baseline Scenarios

The distribution coefficient, K_d, represents the partitioning of the contaminant between the solid and the aqueous phase. As the value of K_d increases the concentration of the contaminant in the sorbed phase increases and the concentration of the contaminant in the aqueous phase decreases. In the model, as the value of the clay K_d is increased the concentration of the dissolved contaminant measured at the downgradient observation point decreases because more of the contaminant is in the sorbed phase in the low permeability clay layer. This increase in sorbed phase concentration leads to a decrease in the "back diffusion" of the aqueous phase out of the low permeability clay after the original TCE source is depleted. This can be seen in the breakthrough curves plotted in Figure 7 for the three values of K_d chosen; as K_d increases, the concentration at which "tailing" occurs decreases. In fact, for the highest value of K_d used in the analysis, the

concentration of the tail is below the MCL for TCE. Note, however, that since more contaminant is stored in the low conductivity layer when K_d is increased, ultimately more will be released. This effect will be quantified when we calculate the first moment of the breakthrough curves for different values of K_d in Section 4.4.

The next sensitivity analysis examines the first order mass transfer rate constant (ζ). Values of 0.01 d^{-1}, and 0.5 d^{-1} are chosen and the breakthrough curves generated are compared to the breakthrough curves for the baseline scenarios. Baseline parameter values for K_d and θ_m of 0.051 m^3-kg^{-1} and 0.1 respectively were used. Figure 8 depicts the breakthrough curves for the ζ sensitivity analysis along with the breakthrough curves for the baseline scenarios.

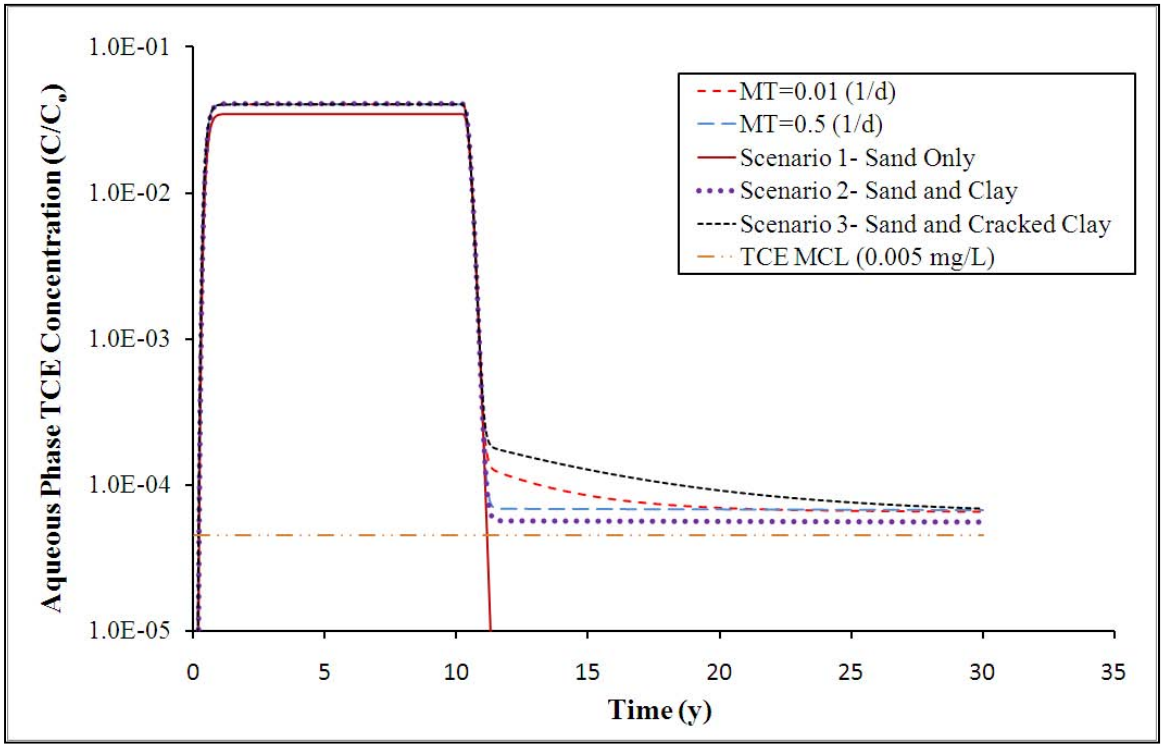

Figure 8: Breakthrough Curves for ζ Sensitivity Analysis along with Baseline Scenarios (MT = -Mass Transfer)

ζ represents the mass transfer rate between the mobile and immobile domains. As the value of ζ is increased, contaminant mass is transferred more quickly from the cracks in the clay (the mobile domain) to the clay (the immobile domain). This increase in mass transfer leads to an increase in contaminant mass stored in the clay which results in a lower aqueous phase TCE concentration downgradient after the TCE source is depleted. As ζ decreases and mass transfer slows, more mass remains in the mobile domain, so higher concentrations of dissolved TCE back diffuse initially, when the DNAPL source is removed. Ultimately, as may be seen qualitatively by looking at Figure 8, since the value of K_d is the same for the three values of ζ, the first moments of the breakthrough curves are the same. This phenomenon has been recognized by a number of investigators (e.g., Valocchi, 1985; Goltz and Roberts, 1986).

The last sensitivity analysis varies the mobile porosity, θ_m, of the clay. Mobile porosity values of 0.01, and 0.5 are chosen and the breakthrough curves generated are compared to the breakthrough curves for the baseline scenarios. Baseline parameter values for K_d and and ζ of 0.051 m^3-kg^{-1} and 0.005 d^{-1} respectively were used. Figure 9 depicts the breakthrough curves for the θ_m sensitivity analysis.

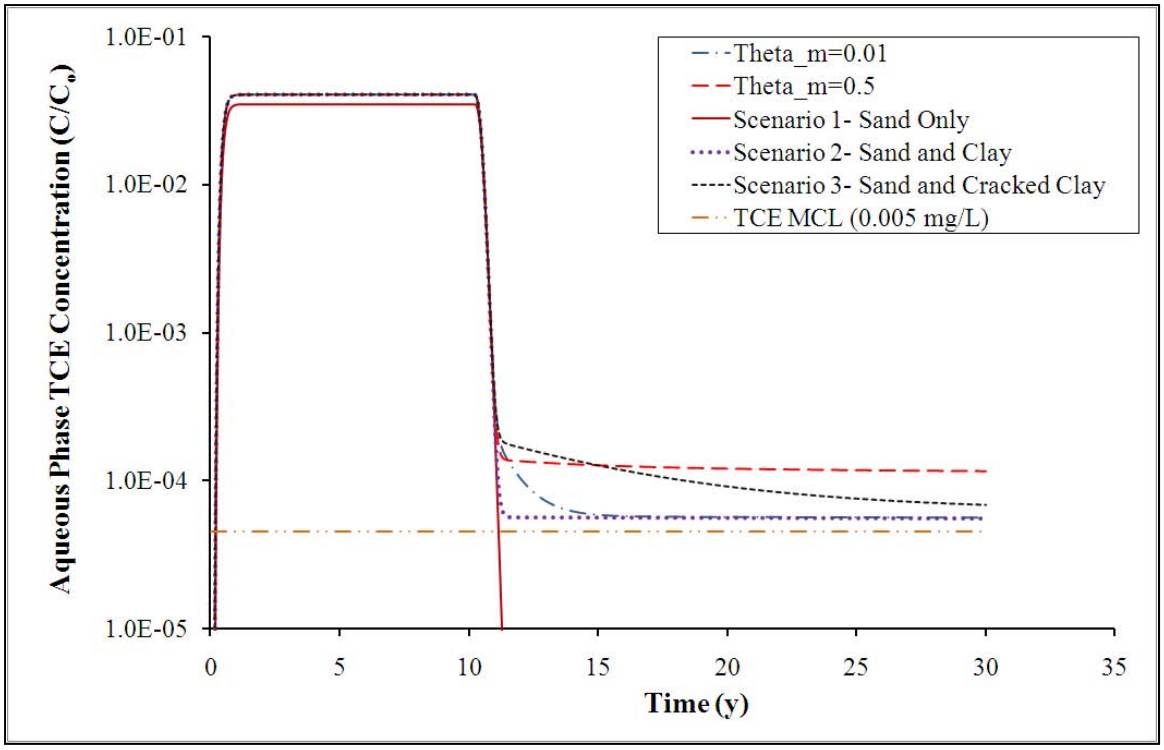

Figure 9: Breakthrough Curves for Clay θ_m Sensitivity Analysis along with Baseline Scenarios

For this research cracks in the clay are represented by θ_m. As the value of the clay θ_m increases the number of cracks in the clay increases. The cracks in the clay lead to "enhanced diffusion" of the aqueous phase TCE into the clay from the DNAPL source on the surface of the clay. This "enhanced diffusion" process ultimately leads to an increase in the contaminant mass stored in the clay as compared to the contaminant mass stored in uncracked clay. Upon depletion of the DNAPL source, the contaminant mass is transported from the clay into the sand aquifer by "back diffusion" and then downgradient by advection. This is demonstrated by comparing the breakthrough curve for Scenario 2 which is the breakthrough curve for uncracked clay (θ_m = 0.001) and the breakthrough curve for clay with substantial cracking (θ_m = 0.5). The tail for the breakthrough curve when θ_m equals 0.5 is at a greater concentration than the tail of the

breakthrough curve for the uncracked clay. An increase in θ_m simulates an increasing number of cracks, and an increasing number of cracks results in an increase in contaminant mass transported into and stored in the clay (i.e., enhanced diffusion). In turn, the enhanced diffusion leads to increased tailing as contaminant that back diffuses from the clay into the sand aquifer upon depletion of the DNAPL source is transported downgradient by advection.

Table 1 in Chapter 3 provides supporting evidence for the idea that as θ_m increased the number of cracks in the clay increased. As Table 1 shows as θ_m increased from 0.01 to 0.5 the number of cracks in the clay increased from 341,239 to 375,292. Also shown in Table 1 is the fact that as θ_m increased from 0.01 to 0.5 the radius of the cracks (b) increased from 0.005 m to 0.027 m and the half distance between the cracks (B) decreased from 0.047 m to 0.033 m. These results are consistent with the fact that as θ_m of the clay increased more cracks formed and the half distance between the cracks must decrease to accommodate the increasing number of cracks formed.

4.4 First Moment Analysis

A moment analysis was conducted and the results compared for K_d values of 0.051 m^3-kg^{-1} and 0.102 m^3-kg^{-1}. The analysis used the baseline values for θ_m and ζ of 0.1 and 0.005 d^{-1} respectively. This analysis was conducted to verify that, the appearance of Figure 7 notwithstanding, ultimately the extent of tailing of a breakthrough curve with a high K_d is greater than for a lower K_d. Mathematically this may be accomplished by calculating and comparing the values of the first moment for each K_d value.

The first moment represents the mean residence time of the solute molecules in the system. As the value of K_d increases more solute is in the sorbed phase and less solute is in the dissolved aqueous phase. This leads to an increased solute residence time in the system and a higher first moment value. As the value of K_d decreases more solute is in the dissolved aqueous phase which leads to a decrease of the residence time in the system and a lower first moment value.

As expected, and belying the appearance of Figure 7, for a K_d of 0.051 m^3-kg^{-1} the first moment is approximately 1,113 years compared to the first moment of 1,259 years for a K_d of 0.102 m^3-kg^{-1}.

5.0 Conclusion and Recommendations

5.1 Conclusion

The primary objective of the research was to model the effects that cracks have on the storage and transport of dissolved aqueous phase CAHs into and out of the low permeability layers, and simulate how this might affect the evolution and longevity of dissolved phase plumes. The dual-domain model developed in this work was used to simulate cracks that might form in the low permeability clay due to the presence of DNAPL. These cracks allow "enhanced diffusion" of aqueous phase CAHs into the clay which leads to increased contaminant mass stored in the clay. This mass stored in the clay then "back diffuses" out of the clay after the DNAPL source is removed creating a dissolved phase contaminant plume that exists long after the DNAPL source is removed. Based on the model results, we found that:

1) as the number of cracks in the clay increases, "back diffusion" out of the clay after the DNAPL source is removed increases, and a higher downgradient concentration tail persists long after the DNAPL source is removed.

2) as the aqueous phase concentration in the clay increases and the sorbed phase concentration decreases a higher downgradient concentration tail persists long after the DNAPL source is removed due to increased "back diffusion" out of the clay.

3) when the sorbed phase concentration in the clay is significantly higher than the aqueous phase concentration, "back diffusion" out of the clay is not significant which could lead to measured downgradient concentrations that are below regulatory limits.

4) upon removal of a DNAPL source pooled atop a low permeability clay layer the "back diffusion" of the aqueous phase CAH out of the clay can cause downgradient plume persistence long after the DNAPL source is removed.

5) remediation strategies that focus only on the removal of the DNAPL source and do not take into account "back diffusion" out of the low permeability clay may fail to meet site cleanup targets and goals.

6) the model has the potential to be used by site remediation managers to guide them in their decision making process on ways to best manage sites requiring remediation.

5.2 Recommendations for Future Research

The current research assumes that aqueous phase CAH is transported from the DNAPL source into the cracks in the clay by advection. Future work should consider the possible impact of DNAPLtransport into the cracks. Clearly, this will result in more contaminant mass in the low permeability layers. The plausibility of this scenario depends upon such factors as the entry pressure required for DNAPL to enter a crack, which in turn would depend upon the crack diameter.

Another recommendation is to use mobile porosity and hydraulic conductivity values for clay from an actual site that has been in contact with "real" DNAPL (containing impurities). These experimental values could be used as input parameters in the model developed for this study.

Other recommendations include incorporation of contaminant degradation in the clay which could lead to a lower contaminant concentration that "back diffuses" out of the clay, two-dimensional laboratory experiments to validate the model, investigation of

other models that could be used to simulate cracking in the clay, development of a model that would allow for cracks to form over time, rather than assume that the cracks develop instantaneously upon arrival of the contaminant source, and finally modeling a “real world” remediation scenario would help with model validation.

Bibliography

Air Force Center for Engineering and the Environment (AFCEE). *AFCEE Source Zone Initiative Final Report*. Brooks Air Force Base, TX, 2007.

Ayral, D., A.H. Demond, M.N. Goltz, and J. Huang. Impact of chlorinated solvents on the structure of clay in low permeability zones in groundwater contamination source areas. *Strategic Environmental Research Program.* 2010.

Ball, W.P., C. Liu, G. Xia, and D.F. Young. A diffusion-based interpretation of tetrachloroethane and trichloroethene concentration profiles in a groundwater aquitard. *Water Resource Resources*. 33(12): 2741-2757, 1997.

Brown, K.W. and J.C. Thomas. A mechanism by which organic liquids increase the hydraulic conductivity of compacted clay minerals. *Soil Sci. Soc. Am. J.* 51(6): 1451-1459, 1987.

Chapman, S.W. and B.L. Parker. Plume persistence due to aquitard back diffusion following dense nonaqueous phase liquid source removal or isolation. *Water Resources Research*. 41: W12411, 2005.

Clark, M. *Transport Modeling for Environmental Engineers and Scientists*. John Wiley and Sons, 2009.

Fookes, P.G. and B. Denness. Observational studies on fissure patterns in cretaceous sediments of south-east england. *Géotechnique*. 19(4): 453-477, 1969.

Goltz, M. N. and P. V. Roberts. Using the method of moments to analyze three-dimensional diffusion-limited solute transport from temporal and spatial perspectives. *Water Resources Research*. 23(8): 1575-1585, 1987.

Goltz, M.N. and P.V. Roberts. Simulations of physical nonequilibrium solute transport models: Application to a large-scale field experiment. *Journal of Contaminant Hydrology*. 3(1): 37-63, 1988.

Grisak, G.E. and J.F. Pickens. Solute transport through fractured media 1. the effect of matrix diffusion. *Water Resources Research*. 16(4): 719-730, 1980.

Harrison, B., E.A. Sudicky, and J.A. Cherry. Numerical analysis of solute migration through fractured clayey deposits into underlying aquifers. *Water Resources Research*. 28(2): 515-526, 1992.

Heiderscheidt, Jeff. Personal Communication. August 2010.

Johnson, R., J. Cherry, and J. Pankow. Diffusive contaminant transport in natural clay: a field example and implications for clay-lined waste disposal sites. *Environ. Sci. Technol.* 23(3): 340-349, 1989.

Kueper, B.H. and D.B. McWhorter. The behavior of dense, nonaqueous phase liquids in fractured clay and rock. *Ground Water*. 29(5): 716-728, 1991.

Li, J., J.A. Smith, and A.S. Winquist. Permeability of earthen liners containing organobentonite to water and two organic liquids. *Environ. Sci. Technol.* 30: 3089-3093, 1996.

Liu, C. and W.P. Ball. Back diffusion of chlorinated solvent contaminants from a natural aquitard to a remediated aquifer under well controlled field conditions: predictions and measurements. *Ground Water*. 40(2): 175-184, 2002.

Mackay, G.M., R.D. Wilson, M.J. Brown, W.P. Ball, D.P. Durfee, G.Xia, and C. Liu. A controlled field evaluation of continuous versus pulsed pump-and-treat remediation of a VOC-contaminated aquifer: Site characterization, experimental setup, and overview of results. *Journal of Contaminant Hydrology*. 41(1): 81-131, 2000.

Parker, B.L, S.W. Chapman, and M.A. Guilbeault. Plume persistence caused by back diffusion from thin clay layers in a sand aquifer following TCE source-zone hydraulic isolation. *Journal of Contaminant Hydrology*. 102: 86-104, 2008.

Parker, B.L, J.A. Cherry, and S.W. Chapman. Field study of TCE diffusion profiles below DNAPL to assess aquitard integrity. *Journal of Contaminant Hydrology*. 74: 197-230, 2004.

Parker, B.L., R.W. Gillham, and J.A. Cherry. Diffusive disappearance of immiscible-phase organic liquids in fractured geologic media. *Ground Water*. 32(5): 805-820, 1994.

Reynolds, D.A. and B.H. Kueper. Numerical examination of the factors controlling DNAPL migration through a single fracture. *Ground Water*. 40(4): 368-377, 2002.

Rowe, R.K and J.R. Booker. Contaminant migration through fractured till into an underlying aquifer. *Can. Geotech. J.* 27: 484-495, 1990.

Sale, T.C., J.A. Zimbron, and D.S. Dandy. Effects of reduced contaminant loading on downgradient water quality in an idealized two-layer granular porous media. *Journal of Contaminant Hydrology*. 102: 72-85, 2008.

SERDP. *Environmental Restoration- ERSON-10-02-The Impact of Contaminant Storage in Low-Permeability Zones on Chlorinated Solvent Groundwater Plumes*. [online].

Retrieved 29 Aug 2010, from: <http://www.serdp.org/Funding-Opportunities/SERDP-Solicitations/Past-Statements-of-Need-SONs/%28language%29/eng-US>

U.S. EPA. *Superfund: EPA Introduces Comprehensive Website on Cleanup of DNAPLs*. [online]. Retrieved 1 August 2010, from: <http://www.epa.gov/superfund/accomp/news/cleanup_dnapl.htm>

Valocchi, A.J. Validity of the local equilibrium assumption for modeling sorbing solute transport through homogeneous soils. *Water Resources Research*. 21(6): 808-820, 1985.

Wilson, J.L. Removal of aqueous phase dissolved contamination: non-chemically enhanced pump-and-treat. *In*: C.H. Ward, J.A. Cherry, and M.R. Scalf, (eds). *Subsurface Restoration*, Chelsea: Ann Arbor Press, 271-285, 1997.

Zheng, C and P. Wang. *Contract Report SERDP-99-1: MT3DMS: A Modular Three-Dimensional Multispecies Transport Model for Simulation of Advection, Dispersion, and Chemical Reactions of Contaminants in Groundwater Systems: Documentation and User's Guide*. Vicksburg, MS, 1999.

REPORT DOCUMENTATION PAGE

Form Approved
OMB No. 074-0188

1. REPORT DATE *(DD-MM-YYYY)*	**2. REPORT TYPE**	**3. DATES COVERED** *(From – To)*
24-03-2011	Master's Thesis	March 2010 to March 2011

4. TITLE AND SUBTITLE
Modeling Enhanced Storage of Groundwater Contaminants Due to the Presence of Cracks in Low Permeability Zones Underlying Contaminant Source Areas

5a. CONTRACT NUMBER

5b. GRANT NUMBER

5c. PROGRAM ELEMENT NUMBER

6. AUTHOR(S)
Miniter, Jeremy M., Captain, USAF

5d. PROJECT NUMBER
JON 11V193

5e. TASK NUMBER

5f. WORK UNIT NUMBER

7. PERFORMING ORGANIZATION NAMES(S) AND ADDRESS(S)
Air Force Institute of Technology
Graduate School of Engineering and Management (AFIT/EN)
2950 Hobson Way
WPAFB OH 45433-7765

8. PERFORMING ORGANIZATION REPORT NUMBER
AFIT/GES/ENV/11-M02

9. SPONSORING/MONITORING AGENCY NAME(S) AND ADDRESS(ES)
Dr. Andrea Leeson
Strategic Environmental Research and Development Program
901 N. Stuart St., Ste 303
Arlington, VA 22203
Phone: 703-696-2118
E-Mail: Andrea.Leeson@osd.mil

10. SPONSOR/MONITOR'S ACRONYM(S)
SERDP

11. SPONSOR/MONITOR'S REPORT NUMBER(S)

12. DISTRIBUTION/AVAILABILITY STATEMENT
APPROVED FOR PUBLIC RELEASE; DISTRIBUTION UNLIMITED

13. SUPPLEMENTARY NOTES
This material is declared a work of the U.S. Government and is not subject to copyright protection in the United States

14. ABSTRACT
Throughout DoD, chlorinated aliphatic hydrocarbons (CAHs), a type of Dense Non-Aqueous Phase Liquid (DNAPL), have been frequently used. In the subsurface, spilled DNAPLs may pool atop low permeability clay layers. In this study a numerical model is constructed using the Groundwater Modeling System to assess how cracks in the clay, either pre-existing or the result of DNAPL-clay interactions, might impact a dissolved CAH plume generated by the DNAPL source. The conceptual model posits a DNAPL source in a high permeability sand aquifer sitting atop a low permeability clay layer. The model assumes dissolved CAH generated by the DNAPL is transported by advection, dispersion, and sorption in the sand. These transport processes are coupled to processes in the clay. In the clay, dissolved CAH is transported by diffusion. However, due to cracks in the clay; "enhanced diffusion" of dissolved CAH by advection may also occur. Advective transport in the cracks coupled to diffusive transport in the clay matrix is simulated using a dual domain model. Modeling indicates that as cracking increases, mass of contaminant in the clay increases. This leads to higher concentrations of contaminant "back diffusing" out of the clay and higher downgradient concentrations long after source removal.

15. SUBJECT TERMS
DNAPL, low permeability clay, back diffusion, enhanced diffusion, Groundwater Modeling System (GMS), dissolved phase plume, dual domain model

16. SECURITY CLASSIFICATION OF:			**17. LIMITATION OF ABSTRACT**	**18. NUMBER OF PAGES**	**19a. NAME OF RESPONSIBLE PERSON**
a. REPORT	**b. ABSTRACT**	**c. THIS PAGE**			MARK N. GOLTZ, ENV
U	U	U	UU	61	**19b. TELEPHONE NUMBER** *(Include area code)* (937) 255-3636, ext 4638

Standard Form 298 (Rev. 8-98)
Prescribed by ANSI Std. Z39-18

Form Approved
OMB No. 074-0188